Geofísica Internacional (1995), Vol. 34, Num. 1, pp. 3-22

Petrology and geochemistry of the Teloloapan subterrane: a Lower Cretaceous evolved intra-oceanic island-arc

Oscar Talavera Mendoza, Joel Ramírez Espinosa and Martín Guerrero Suástegui
Escuela Regional de Ciencias de la Tierra, Universidad Autónoma de Guerrero, Taxco, Gro., México.

Received: August 4, 1993; accepted: September 29, 1994.

RESUMEN

Al sur del Eje Volcánico Mexicano, el subterreno Teloloapan constituye una de las secuencias tectonoestratigráficas incluidas en el superterreno Guerrero. Este subterreno incluye una unidad basal esencialmente volcánica de edad Hauteriviano-Aptiano (formación Villa Ayala), compuesta en su mayoría por basaltos y localmente por andesitas y riolitas. Esta unidad es sobreyacida por una unidad de volcaniclásticos de edad Aptiano superior (formación Acapetlahuaya), una unidad de calizas arrecifales (formación Teloloapan) y calizas detríticas finas (formación Amatepec) del Albiano-Cenomaniano inferior y finalmente por una unidad de lutitas y areniscas (formaciones Pachivia/Miahuatepec) de edad post-Cenomaniano inferior. Las rocas volcánicas muestran características petrográficas, mineralógicas, geoquímicas e isotópicas típicas de las series calco-alcalinas: (i) presencia de basaltos y andesitas de dos piroxenos y anfíbol; (ii) cristalización temprana de los óxidos de Fe-Ti; (iii) composición de los clinopiroxenos; (iv) comportamiento del Fe durante la diferenciación; (v) concentraciones elevadas en HFSE y en LREE; (vi) relaciones $(La/Yb)_N$ elevadas; y, (vii) valores de ε_{Nd} bajos. Las características petrológicas, geoquímicas e isotópicas son compatibles con un origen en un arco de islas intra-oceánico. Comparadas con las rocas calco-alcalinas intra-oceánicas primitivas, las rocas de Teloloapan están enriquecidas en HFSE (Y, Nb, Zr y en menor grado TiO_2) y en HREE. Estas características son comparables con las observadas en las series calco-alcalinas medianamente ricas y ricas en K de arcos intra-oceánicos maduros como las series calco-alcalinas de los arcos de Sunda o Antillas Menores. Se sugiere que las lavas de Teloloapan reflejan diversos procesos magmáticos como la fusión parcial de una fuente mantélica ligeramente enriquecida modificada por sedimentos pelágicos subductados y posteriormente por cristalización fraccionada y/o acumulación cristalina.

PALABRAS CLAVE: Terreno Guerrero, Subterreno Teloloapan, Cretácico inferior, calco-alcalino, arco intra-oceánico, fuente mantélica enriquecida, cristalización fraccionada.

ABSTRACT

The Teloloapan subterrane is a tectonostratigraphic sequence in the composite Guerrero Terrane. It includes an Hauterivian to Aptian, essentially volcanic unit (Villa Ayala formation) composed predominantly of basalts overlain by upper Aptian volcaniclastic turbidites (Acapetlahuaya formation), Albian to lower Cenomanian limestones (Teloloapan and Amatepec formations) and post-lower Cenomanian sandstones and shales (Pachivia/Miahuatepec formations). Volcanics show typical petrographic, mineralogical, geochemical and isotopic characteristics of calc-alkaline suites: (i) presence of two-pyroxene and amphibole basalts and andesites; (ii) early crystallization of Fe-Ti oxides; (iii) clinopyroxene chemistry; (iv) Fe-depletion trend; (v) high concentrations of LILE and LREE; (vi) high $(La/Yb)_N$ ratios; and, (vii) low ε_{Nd}. This is compatible with origin in an intra-oceanic island-arc. Compared to primitive intra-oceanic calc-alkaline suites, Teloloapan volcanics are enriched in HFS elements (Y, Nb, Zr and in lesser degree TiO_2) and HREE and are similar to medium- to high-K calc-alkaline suites from evolved intra-oceanic island-arcs, e.g. from the Sunda or Lesser Antilles arcs. We suggest that Teloloapan lavas may reflect partial melting of a slightly enriched mantle source modified by subducted pelagic sediments, and later differentiation by crystal fractionation and/or crystal accumulation.

KEY WORDS: Guerrero terrane, Teloloapan subterrane, lower Cretaceous, calc-alkaline, intra-oceanic island-arc, enriched mantle source, crystal fractionation.

INTRODUCTION

The Guerrero suspect Terrane [previously named Tierra Caliente Complex by Ortega, (1981) or Nahuatl Terrane according to Sedlock *et al.* (1993)] has been divided into three distinctive subterranes on the base of stratigraphic and structural characteristics (Campa *et al.*, 1981; Campa and Coney, 1983). From east to west these are: (1) the Teloloapan subterrane, which borders on the Mixteco Terrane, defined as a highly deformed and slightly metamorphosed volcano-sedimentary arc sequence of Late Jurassic to Late Cretaceous age; (2) the Huetamo subterrane, located in the middle part of the terrane, an undeformed and unmetamorphosed, essentially sedimentary sequence of Late Jurassic to Late Cretaceous age; and, (3) the Zihuatanejo subterrane, cropping out along the Pacific coast, which includes an undeformed and unmetamorphosed volcano-sedimentary arc succession of Early Cretaceous age, overlying a variety of exotic blocks included in a severely deformed matrix of flysch and serpentinite (Figure 1).

Campa *et al.* (1974), De Cserna *et al.* (1978), Campa and Ramírez (1979), De Cserna and Fries (1983) and more recently Guerrero *et al.* (1990, 1991, 1993) and Elías and Sánchez (1992) established with some detail the stratigraphy and the structural history of the Teloloapan volcano-sedimentary sequence. The stratigraphy of the Huetamo sequence has been established in Pantoja's (1959) classical work on the Huetamo-San Lucas region. Finally, the stratigraphy of the Zihuatanejo volcano-sedimentary sequence has been studied in some detail by Boneau (1976), Campa and Ramírez (1979), Vidal *et al.* (1980) and Delgado *et al.* (1990).

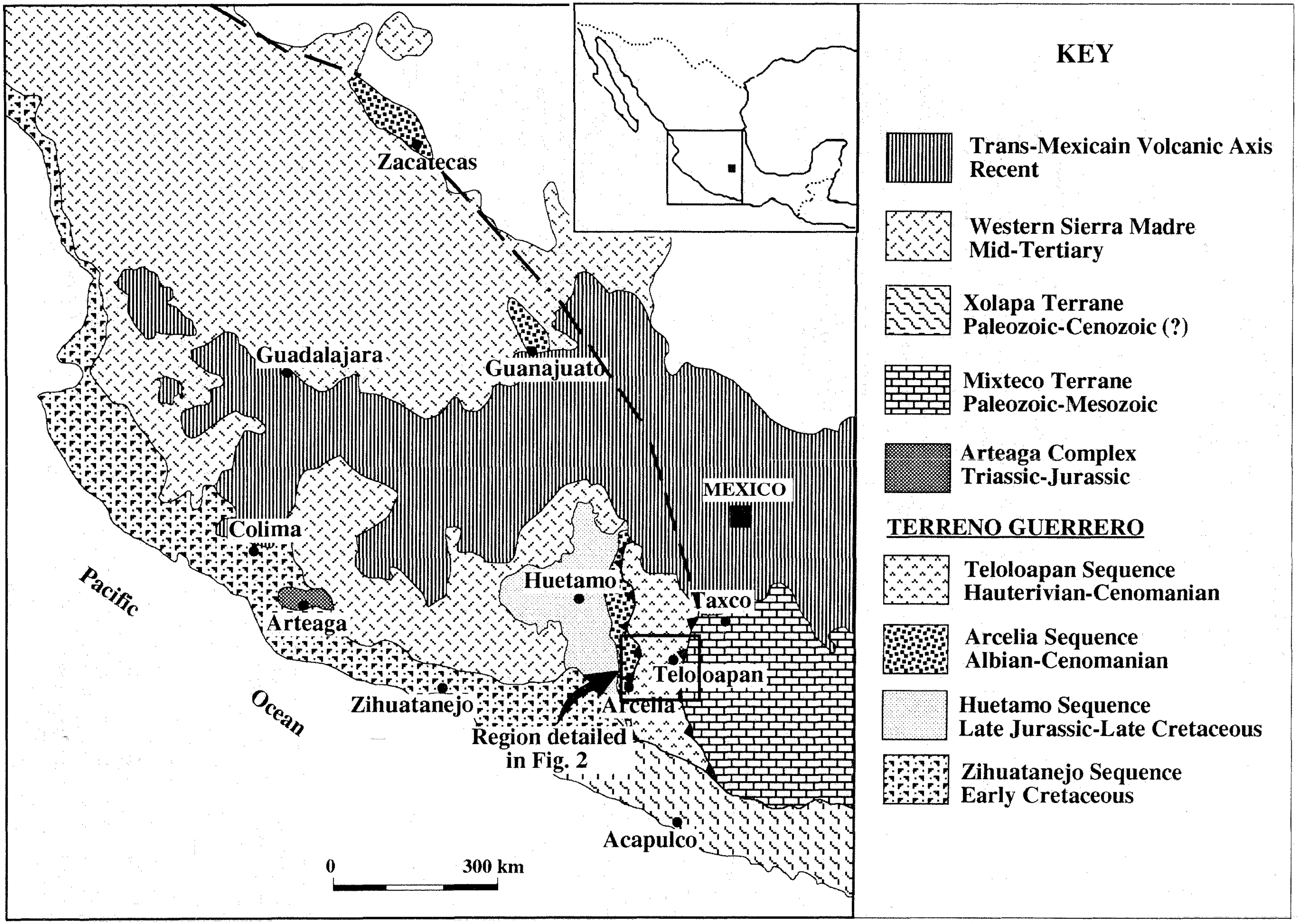

Fig. 1. Simplified structural map of southern Mexico showing tectonostratigraphic sequences constituting the southern half of the Guerrero Terrane (Modified from Campa *et al.*, 1981).

In contrast with the great number of studies concerning the stratigraphy and the structural evolution, geochemical studies are few and regional in character (Ortiz *et al.*, 1991; Lapierre *et al.*, 1992; Talavera, 1993; Tardy *et al.*, 1993; Centeno *et al.*, 1993). Thus little is known about the tectonomagmatic evolution of each sequence constituting the Guerrero Terrane. This paper presents the results of a detailed petrological and geochemical study including mineral chemistry, major trace and rare-earth elements and $^{87}Sr/^{86}Sr$ and $^{143}Nd/^{144}Nd$ isotopic determinations in lavas of the Teloloapan subterrane sequence. These data as well as recent stratigraphic and sedimentological data help to constrain the magmatic evolution as well as the tectonic setting of the Teloloapan subterrane.

GEOLOGICAL SETTING AND LITHOSTRATIGRAPHIC SUCCESSION OF THE TELOLOAPAN SUBTERRANE

The Teloloapan subterrane (Campa *et al.*, 1981; Campa and Coney, 1983), is more than 300 km long and 80 km wide. It is located in the southeastern limit of the Guerrero Terrane, in the central part of the Cordilleran domain of southern Mexico (Figure 1). The Teloloapan-Arcelia study area is located in the southern half of the Teloloapan subterrane. In this area, three north-trending lithotectonic assemblages, separated by west-dipping, regional faults are exposed (Figures 2 and 3). These assemblages are, from east to west: (1) the Guerrero-Morelos platform formed by Middle to Late Cretaceous carbonate and clastic rocks (Fries, 1960; De Cserna *et al.*, 1978), which forms part of the Mixteco Terrane evolution (Campa *et al.*, 1981; Campa and Coney, 1983; Coney and Campa, 1984; Sedlock *et al.*, 1993); (2) The Teloloapan volcano-sedimentary sequence discussed here; and (3) the Arcelia sequence containing tholeiitic island-arc volcanic and plutonic rocks, black shales and radiolarian cherts of Albian to lower Cenomanian age (Davila and Guerrero, 1990; Delgado *et al.*, 1990; Ortiz *et al.*, 1991). Some pillow basalt with MORB affinity has been reported in the eastern part of the Arcelia sequence (Ortiz, 1992; Talavera, 1993), but the relationships with the tholeiitic island arc assemblage are unknown.

The Teloloapan volcano-sedimentary sequence has been severely affected by a polyphase tectonogenesis involving, at least, two major stages of deformation. Whether these stages are a product of a single, extended deformation event (Laramide orogeny; Salinas *et al.*, 1992; Monod *et al.*, 1992) or of two distinctive events (Oregonian and Laramide orogenies; Campa *et al.*, 1974; Campa *et al.*, 1976; Tardy, 1980; Ortiz *et al.*, 1991; Lapierre *et al.*, 1993) is unresolved. Deformation produced a complex pattern of east-vergent isoclinal folds associated with penetrative foliation and thrust faulting (De Cserna *et al.*, 1978; Campa and Ramírez, 1979; Tardy, 1980). As a result, repetitions in the stratigraphic column and stratigraphic inversions are common, and the whole stratigraphic succession is difficult to establish from a single cross section.

The region has been studied by a number of workers in the last two decades (*e.g.*, Campa *et al.*, 1974; De Cserna *et al.*, 1978; Campa and Ramírez, 1979; De Cserna and Fries, 1981; Guerrero *et al.*, 1990, 1991; Elías and Sánchez, 1992). The lithostratigraphic correlation chart of the Teloloapan region shows the four main lithostratigraphic columns proposed at present (Figure 4).

According to Guerrero *et al.* (1990; see Figure 4, column 3, and Figure 5), the base (Villa Ayala formation) is represented by more than three kilometers of basic to intermediate, pillowed or massive lavas, pillow breccias and hyaloclastites, which are interbedded in the lower levels with Early Cretaceous radiolarian siliceous sediments, and at the top with coarse-grained volcanic conglomerates and debris flow deposits containing Aptian fauna (Guerrero *et al.*, 1990; 1991). Some discontinuous strata of reefal limestone are mixed or interbedded with volcanic and volcaniclastic rocks in the top levels of the volcanic succession. This informal lithostratigraphic unit was described previously by Campa *et al.* (1974) as the lower volcanic member of the Late Jurassic-Early Cretaceous "Secuencia Volcánica-Sedimentaria Metamorfizada de Ixtapan de la Sal-Teloloapan". Others (*e.g.*, De Cserna *et al.*, 1978; De Cserna and Fries, 1981; Elías and Sánchez, 1992) correlated this unit with part of the "Roca Verde Taxco Viejo" and Taxco Schist cropping out approximately 100 km east of the study region and considered, respectively, as Triassic and Late Precambrian-Early Paleozoic in age (Figure 4). Recently, Elías and Sánchez (1992) considered this unit as part of the regional basement and assigned it a Permian to Triassic age.

The volcanic unit is covered by a 1500 m thick sequence consisting of three informal units (Figures 4 and 5): (1) a unit of greywacke and tuffaceous shale turbidites (Acapetlahuaya formation); (2) a unit of reefal limestones and related carbonated debris flow deposits (Amatepec and Teloloapan formations); and, (3) a unit of flysch-like sandstone and shale deposits (Pachivia and Miahuatepec formations). Primary contacts between units are always transitional and lateral facies changes are common. The age of the sedimentary succession, based on numerous paleontologic determinations, ranges from Aptian to Cenomanian (Campa and Ramírez, 1979; Guerrero *et al.*, 1990, 1991). These units were described by Campa *et al.* (1974) as the upper sedimentary member of their "Secuencia Volcánica-sedimentaria Metamorfizada de Ixtapan de la Sal-Teloloapan". De Cserna *et al.*, (1978), De Cserna and Fries, (1981) and Elías and Sánchez, (1992) considered some of these units either as part of the Taxco Schist or as part of the Middle to Late Cretaceous Guerrero-Morelos Platform cropping out immediately East of the study area (cf. Figure 1). In particular, the greywacke and tuffaceous shale turbidites (Acapetlahuaya formation) were correlated with the Taxco Schist whereas the unit of reefal limestone and related carbonated debris flow deposits (Amatepec and Teloloapan formations) were assigned to the Morelos, Amatepec and/or Xochipala Formations. Finally, the unit of flysch-like sandstone and shale deposits (Pachivia-Miahuatepec formations) has been commonly correlated with the Mexcala and/or Mal Paso Formations.

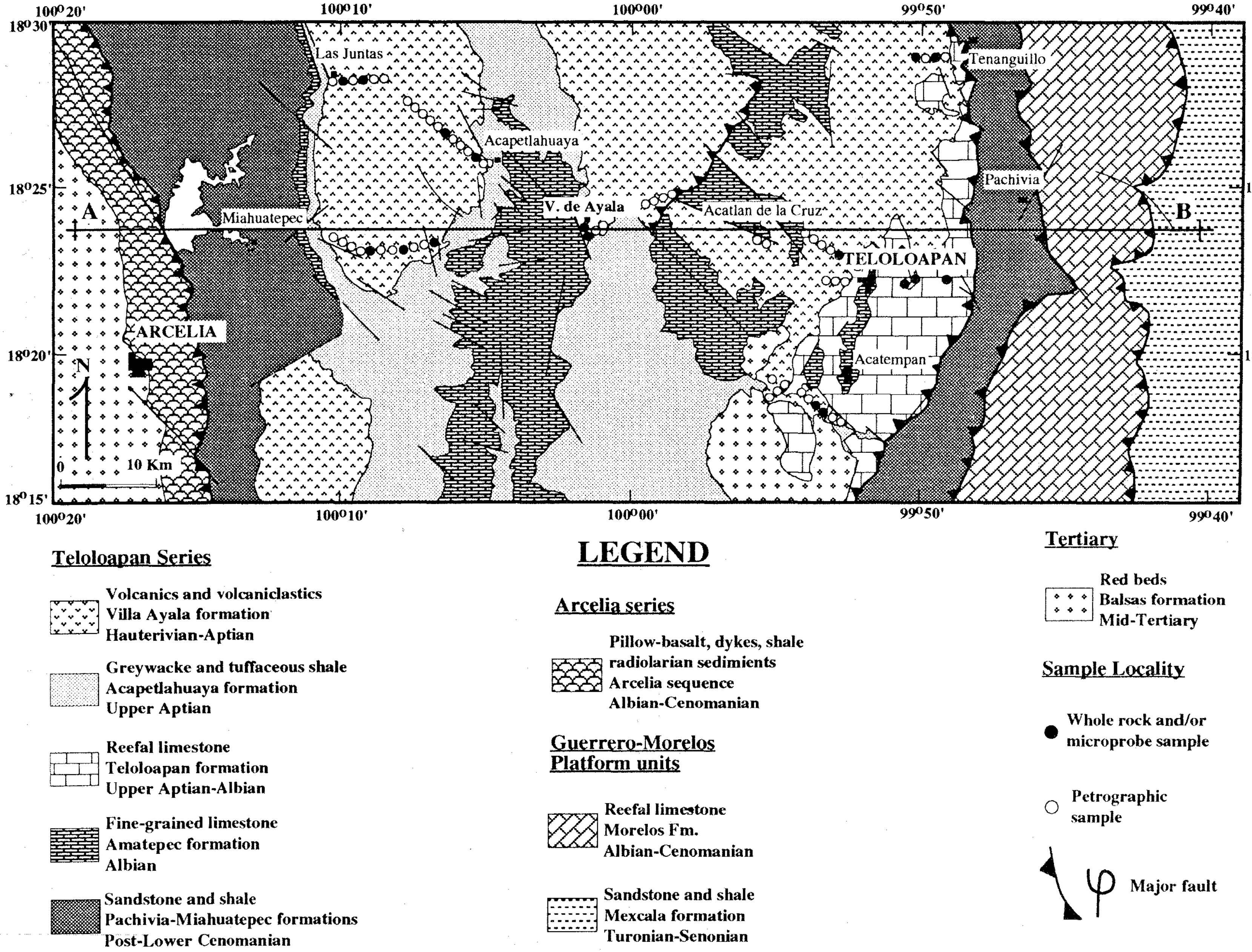

Fig. 2. Geological map of the southern half of the Teloloapan subterrane in the Arcelia-Teloloapan area showing sampling localities (After Ramírez*et al.*, 1991). A-B line represent location of cross section presented in Figure 3.

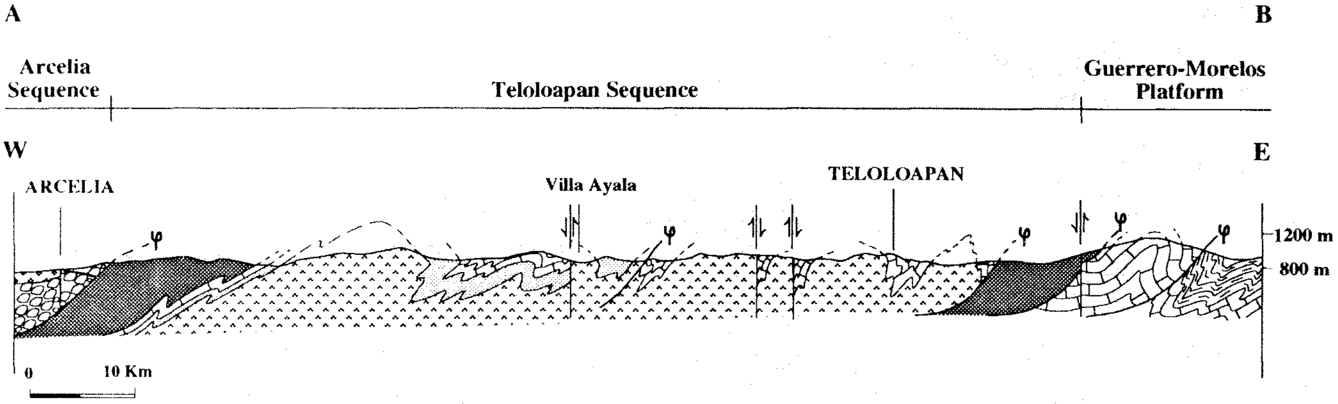

Fig. 3. Regional structural section across the Teloloapan subterrane showing the relationships between the Teloloapan series and the Arcelia and Guerrero-Morelos units. For symbols see Figure 2.

METODOLOGY AND ANALYTICAL TECHNIQUES

Volcanic rocks were systematically sampled based on thickness of flows, phenocryst types and contents and colour variations (Figure 2). About 250 samples were studied under the polarizing microscope. Twenty samples, representative of all recognized petrographic types and stratigraphic levels, were selected for microprobe analysis and sixteen for major- trace- and rare-earth-elements analysis. Five samples were additionally analyzed for $^{87}Sr/^{86}Sr$ and $^{143}Nd/^{144}Nd$ isotopic compositions.

Mineral compositions were measured in automated CAMEBAX microprobes at the BRGM-Université d'Orléans common laboratory and at ENSEEG, Université Joseph Fourier, Grenoble, France using Albite (Na), K-Feldspar (K), Corindon (Al), Wollastonite (Si), Forsterite (Fe), Apatite (Ca), Chromite (Cr), Rutile (Ti), Rodonite (Mn) and Bunsenite (Ni) and MgO (Mg) as standards. We used constant beam current at 10 na, a 15 kV accelerating potential and spot size at 1-3 µm. Count times were in general 6 to 10s except for Cr for which longer, 20s count times were required. Under these conditions, concentrations below 0.1% were disregarded. Concentrations of major- trace- and rare-earth-elements in whole rock were measured using ICP-MS techniques at the Centre de Recherches Pétrographiques et Géochimiques, Nancy, France. Analytical errors are as follows: 0.1 to 0.3% for major elements; 0.5 ppm for trace elements and REE lower than 10 ppm and 5% for those higher than 10 ppm. Nb contents are accurate to ±1 ppm based on repeated analyses of JB1, JB2 and SPX standards (XRF and ICP-MS). Sr and Nd isotopic determinations were carried out by isotopic dilution in a CAMECA TST 206 at the Laboratoire de Géochimie Isotopique, Clermont-Ferrand, France using techniques described by Alibert *et al.* (1983) and Michard *et al.* (1985). Values of used standards are: E & A = 0.70799 ± 4 and BCR = 0.51264 ± 3. Analytical limits are 2σ.

PETROGRAPHY OF LAVAS AND MINERAL CHEMISTRY

(a) Petrography

Prior to this study, most workers had considered Teloloapan volcanic rocks to be essentially andesites based on field observations and/or modal compositions (*e.g.* Campa *et al.*, 1974; De Cserna *et al.*, 1978; Campa and Ramírez, 1979; De Cserna and Fries, 1981). However, whole rock analysis reveals that Teloloapan volcanics are predominantly basalts ($SiO_2 < 53\%$) with locally abundant andesites ($53\% < SiO_2 < 63\%$) and rhyolites ($SiO_2 > 68\%$) [Basaltic Volcanism Study Project, 1981]. All lavas contain metamorphic assemblages ranging in grade from zeolite to greenschist facies. The secondary minerals include laumontite, celadonite, chlorite, prehnite, pumpellyite, epidote, titanite, albite, K-feldspar and actinolite, which commonly fill amygdules and veins or replace primary minerals and groundmass. In spite of the alteration of igneous minerals and groundmass, magmatic textures and structures are in general well preserved suggesting that the transformations might result from hydrothermal, oceanic-type metamorphism (Talavera, 1990; Talavera *et al.*, 1993).

Basalts occur throughout the volcanic sequence, but they are particularly abundant in the lower stratigraphic levels, where they form nearly 100% of volcanic rocks. They show variable textures ranging from aphyric to highly porphyritic with phenocryst content between 0 and 30 volume percent. Aphyric basalts show divergent, intersertal or partly variolitic textures with intergrowths of acicular plagioclase, clinopyroxene and chloritized glass. Acicular oxides were observed in few samples. Porphyritic basalts show seriate and glomeroporphyritic textures with phenocrysts and microphenocrysts of plagioclase, clinopyroxene, orthopyroxene and oxides set in an hypocrystalline to holocrystalline groundmass of plagioclase, clinopyroxene, oxides and intergrowths of chlorite and pumpellyite/epidote derived from the transformation of glass. Both, clinopyrox-

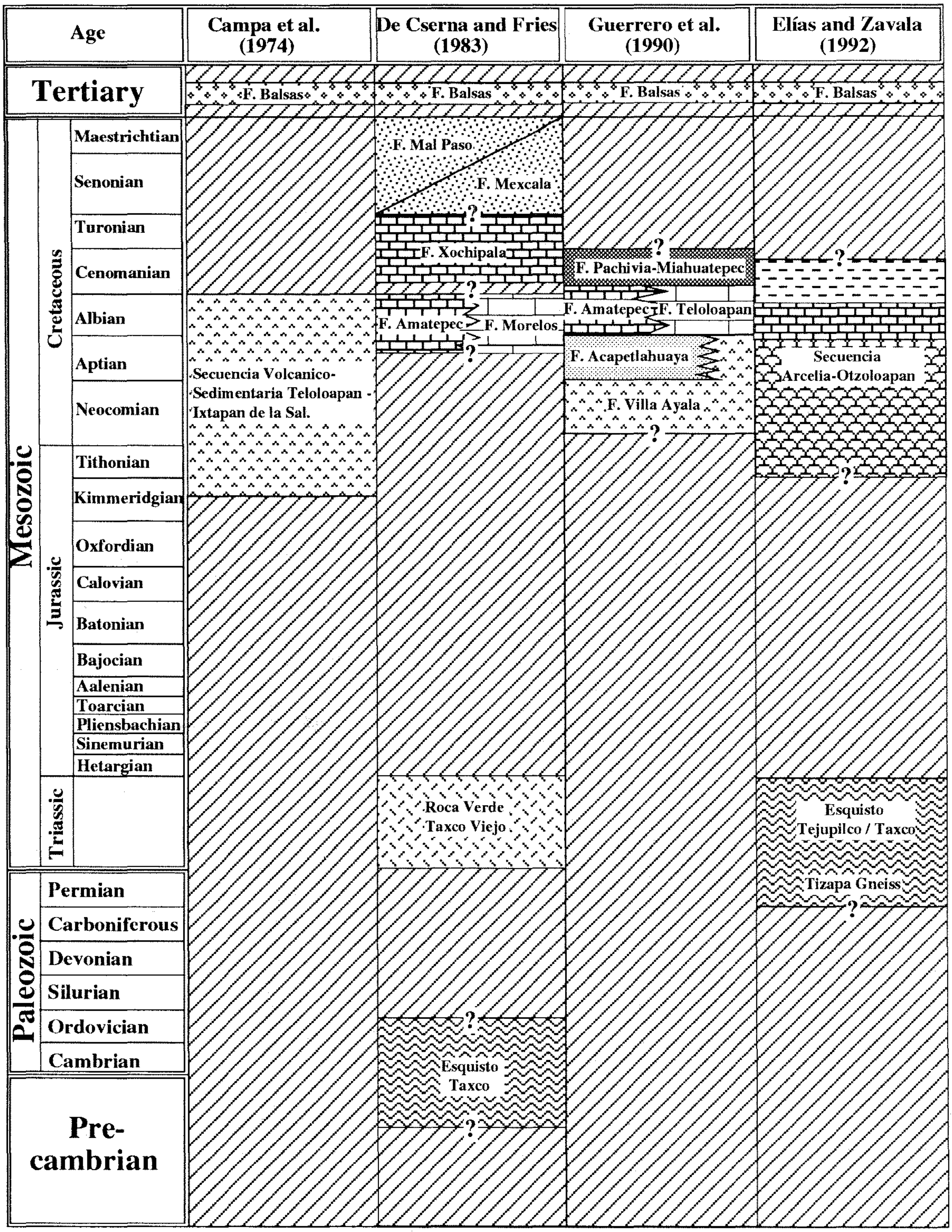

Fig. 4. Lithostratigraphic correlation chart of the Teloloapan formations.

ene and orthopyroxene often contain inclusions of Fe-Ti oxides proving early crystallization of the oxide phases. Olivine phenocrysts were found in some of the bottom basalts whereas amphibole was observed as phenocrysts and more rarely as inclusions in plagioclase megacrysts in some chemically evolved basalts.

Andesites were found only in the upper levels of the volcanic sequence, associated with amphibole- and orthopyroxene-bearing basalts and rare rhyolites. All are highly porphyritic and contain phenocrysts of plagioclase, orthopyroxene, oxides and amphibole set in a groundmass of an intergranular mix of plagioclase laths, acicular oxides,

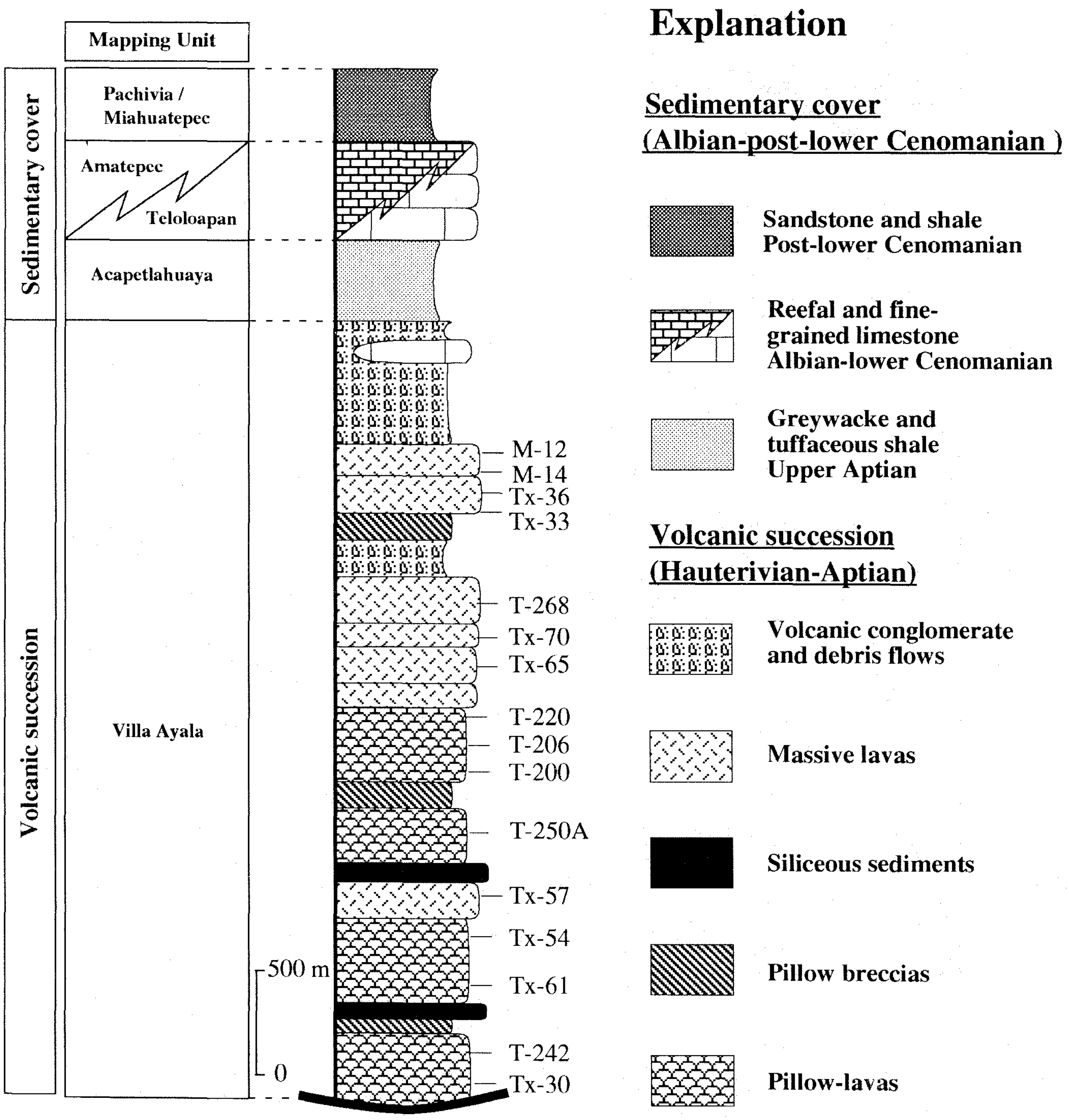

Fig. 5. Lithostratigraphic column of the Teloloapan subterrane sequence according to Guerrero *et al.* (1990) showing location of the sixteen analyzed samples.

orthopyroxene and devitrified glass. Some andesites contain in addition clinopyroxene either as rims around orthopyroxene phenocrysts or as microphenocrysts dispersed in the groundmass.

Rhyolites are essentially aphyric with microgranular to perlitic textures and contain rare microphenocrysts of plagioclase and occasionally amphibole transformed into hematite, chlorite and epidote. The groundmass originally rich in glass is now formed of microcrystalline quartz, plagioclase and K-feldspar.

(b) Mineralogy

Hydrothermal metamorphism has altered considerably the composition of most igneous minerals with the exception of clinopyroxenes, calcic amphiboles and some plagioclases. Olivine and orthopyroxene are completely altered to a microcrystalline mix of chlorite + epidote/pumpellyite + quartz or celadonite + chlorite + quartz and are only recognized by their typical external shapes. Olivine ghosts show typical bi-pyramidal crystals some times with spinel inclusions and reabsorbed margins, whereas orthopyroxenes display typical short prismatic crystals. Fe-Ti oxides are partly transformed in titanite + hematite.

Plagioclase is easily the most abundant phenocryst phase in both basalts and andesites although clinopyroxene is as abundant as plagioclase in the least fractionated basalts. It occurs as subhedral to euhedral phenocrysts up to 0.15 mm in size dispersed in the groundmass, in glomerocryst or as microlites. Plagioclase is partly or completely replaced by albite, K-feldspar and/or laumontite or by an association containing albite, prehnite and epidote or pumpellyite. Primary plagioclase was only recorded in a few acidic andesites from the top stratigraphic levels. Plagioclase phenocrysts show little chemical variation; all fall in the range of An_{40} to An_{45}, whereas microphenocrysts and microlites are slightly more sodic (An_{37-40}) (Table 1).

Clinopyroxene is found in all lavas except in acidic andesites and rhyolites. It generally occurs as euhedral to subhedral crystals up to 0.1 mm, either dispersed in the groundmass or in crystal clusters alone or with plagioclase. In some two-pyroxene basalts and rarely in andesites, clinopyroxene occurs as rims around orthopyroxene phenocryst. It is also a common phase in groundmass of both basalts and andesites as elongated microcrystals associated with plagioclase and acicular oxides.

Clinopyroxene shows a rather wide range of composition (Figure 6). With few exceptions, clinopyroxene in basalts ranges from diopside (Ca_{45-47} Fe_{6-9} Mg_{45-48}) to augite (Ca_{37-45} Fe_{10-25} Mg_{37-47}), whereas in andesites, endiopside (Ca_{41-45} Fe_{7-10} Mg_{47-50}) and augite (Ca_{42-45} Fe_{10-18} Mg_{40-48}) coexist. Rims of some phenocrysts and microlites have compositions of salite (Ca_{45-46} Fe_{10-19} Mg_{28-38}). With the exception of rare phenocrysts and microlites, clinopyroxene is optically zoned with variations in composition from Cr-rich diopsidic or endiopsidic cores to Cr-poor salitic or augitic rims.

Clinopyroxene cores plotted in the discrimination diagrams of Leterrier *et al.* (1982) show orogenic affinities (Figure 7). Ca + Na (cations per structural formula) is considerably lower compared to those currently found in clinopyroxenes of alkali basalts and almost all clinopyroxenes fall in the field of sub-alkali basalts in the Ca + Na-Ti plot (Figure 7a). The sum of Ti + Cr is more variable: although there is an important overlap, the majority of analyses plot in the orogenic field in the Ca-Ti + Cr diagram (Figure 7b). Finally, the total Al and Ti contents indicate calc-alkaline rather tholeiitic affinities (Figure 7c).

It has been suggested that the relative partitioning of Al in the tetrahedral and octahedral sites of clinopyroxenes is sensitive to crystallization pressure. For example, Aoki and Kushiro (1968) found that clinopyroxenes crystallized at high pressure (>10 kb) as eclogites have systematically low (< 0.6) Al^{IV}/Al^{VI} ratios, whereas clinopyroxenes precipitating at low pressure (<6 kb), as in most igneous rocks, have significantly higher (>4.5) Al^{IV}/Al^{VI} ratios. Clinopyroxenes from granulites and inclusions in basaltic rocks (≈4 to 10 kb) have intermediate ratios ($0.6<Al^{IV}/Al^{VI}<4.5$). Analyzed clinopyroxenes are all characterized by high (>1.1; more than 85% are >2.4) Al^{IV}/Al^{VI} ratios suggesting that they have essentially crystallized at low pressure and that fractionation took place likely in the upper levels of the crust.

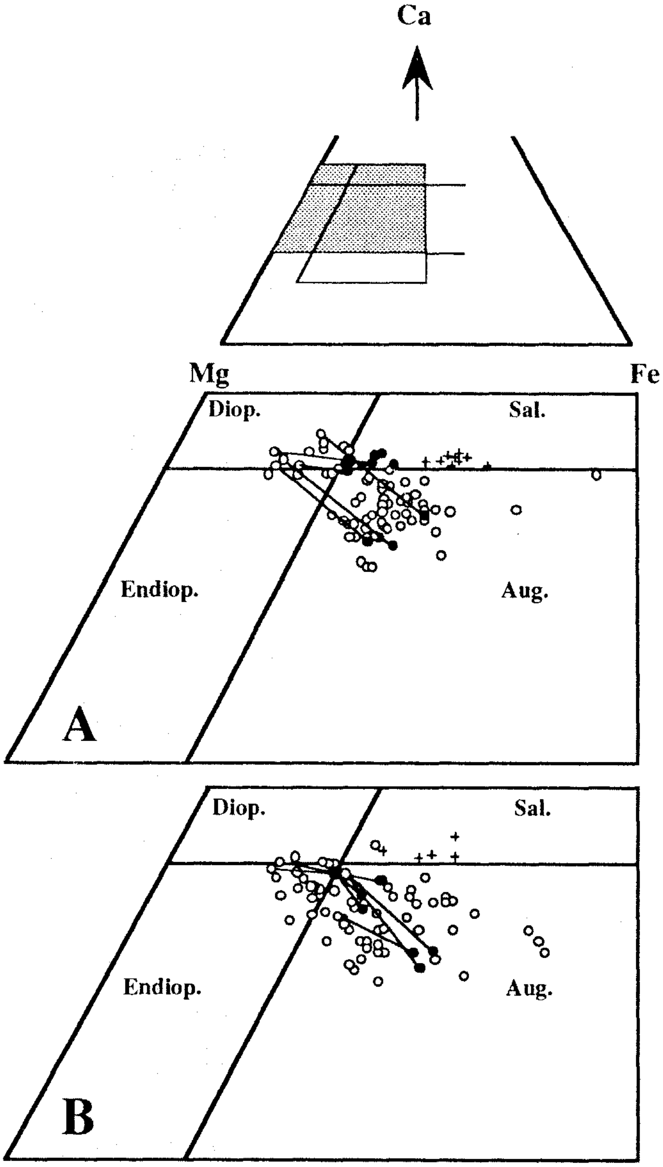

Fig. 6. Clinopyroxene compositions and core-rim variations for basalts (A) and andesites (B) in the diagram Ca-Mg-Fe.

Amphibole is present in some chemically evolved basalts but is particularly abundant in andesites, where it occurs as phenocrysts (up to 0.1 mm) or microphenocrysts (0.01 to 0.1 mm) dispersed in the groundmass, rarely as in-

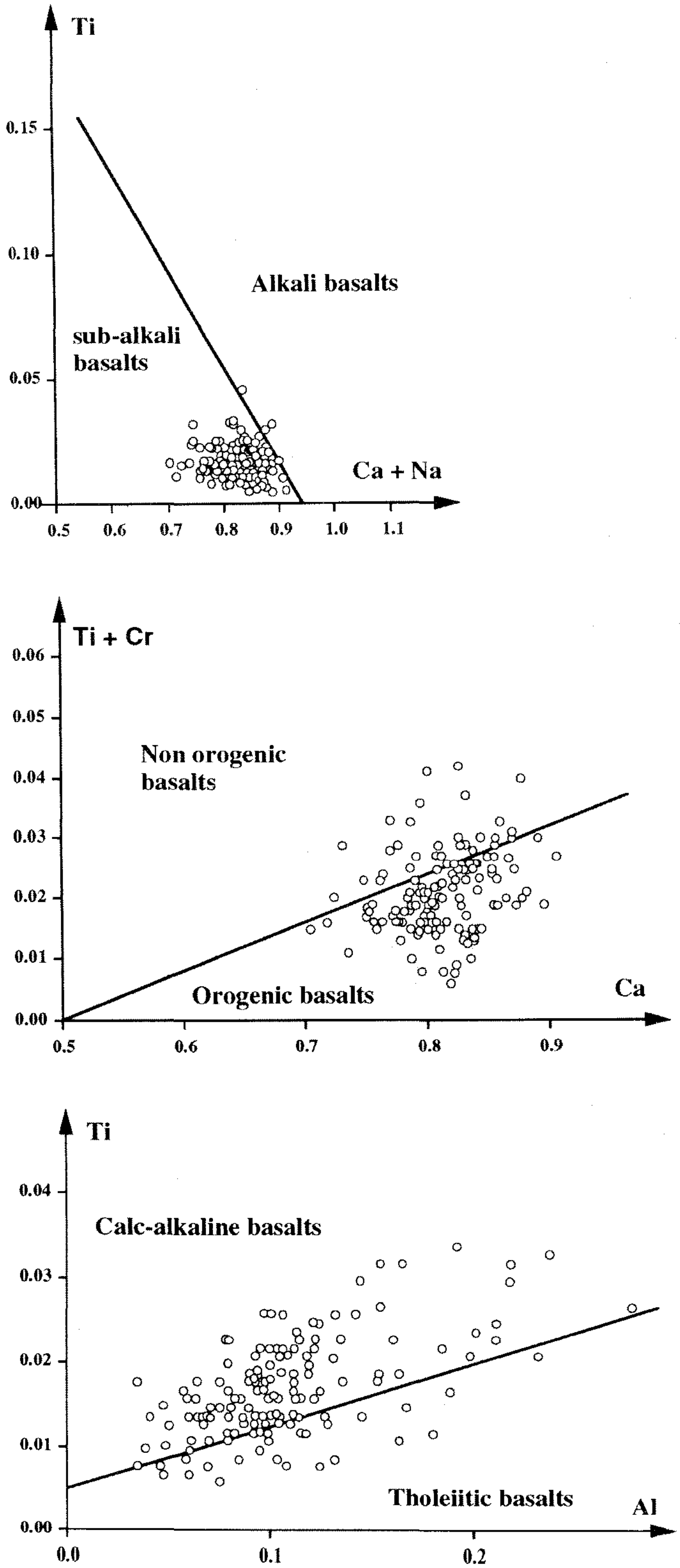

Fig. 7. Identification of the magmatic affinity of the Teloloapan lavas using clinopyroxene analyses in the discrimination diagrams of Leterrier *et al.* (1982).

clusions in plagioclase. It further appears as rims around clinopyroxene phenocrysts suggesting that the magma had increasing water content during differentiation and that this mineral could be formed by reaction of clinopyroxene with hydrous residual melt. According to Leake's (1978) classification scheme (Figure 8), amphiboles range in composition from pargasite through ferroan-pargasite, ferroan-pargasitic hornblende and edenitic hornblende to edenite (structural formulas were calculated on the basis of 23 oxygens assuming total Fe as Fe^{2+}; Table 1). In general, amphibole in basalts tends to be slightly richer in total Al and Mg compared to amphibole of similar composition in andesites. Pargasite is the typical amphibole in basalts but all compositions exist in some andesites (Figure 8). Al^{IV} contents in all amphiboles range from 1.3 to 1.9 and are within the range observed in typical amphibole from island arc andesites (Jakes and White, 1972). In contrast, Al^{VI} content, considered by some workers (Hammarstrom and Zen, 1986; Hollister *et al.*, 1987) as indicative of crystallization pressure, is relatively low suggesting the crystallization of amphibole at low pressure in good agreement with clinopyroxene data. The major exceptions are pargasites in basalts and andesites, with relatively high Al^{VI} contents (Table 1). However, Al-rich pargasites in direct contact with groundmass invariably show evidence of instability such as corroded margins and thus, it is likely that these Al-rich amphiboles represent xenocrysts. On the other hand, nearly all amphiboles are surrounded by a thin (0.03 mm) reaction rim of microgranular oxides or of a mix of oxide ± albitized plagioclase ± clinopyroxene ± actinolite. Since primary compositions of plagioclase and oxides around amphibole are not preserved, it is difficult to say if this association is related to the instability of amphibole at very low pressure as suggested by Stewart (1975), or if rims simply represent partial transformation of amphibole due to metamorphism.

GEOCHEMISTRY AND ISOTOPIC COMPOSITION

Lavas have variable Al_2O_3 (12.3-18.5%) content, which tends to decrease with increasing SiO_2 suggesting extraction of plagioclase from the liquid during differentiation. Similar trends are observed with Fe_2O_3, TiO_2, V and Sc contents, which systematically decrease from basalts through andesites to rhyolites, feature commonly linked to oxide fractionation in calc-alkaline suites (Miyashiro, 1974; Miyashiro and Shido, 1975). All the lavas are depleted in MgO, Cr, Ni and Co indicating that no sample represents the composition of primary mantle-derived magmas and that they all are products of previously differentiated melts (Nicholls and Whitford, 1976; Sato, 1977). The low Mg number (15 to 45) in all samples supports this observation. On the other hand, decreasing MgO, Cr, Ni and Co with increasing SiO_2 strongly suggests an important fractionation of clinopyroxene ± olivine phases.

An extremely large variation in the concentrations of CaO, Na_2O and K_2O and related incompatible elements such as Rb, Ba and Sr is found in lavas even when having similar SiO_2 contents. It is now well known that these elements tend to be mobilized during hydrothermal alterations. Thus the large variations observed in Teloloapan

Table 1

Representative micro-probe analyses of primary minerals of the Teloloapan basalts and andesites. C: core; B: rim; M: microlite.

Mineral	Pg	Pg	Cpx	Cpx	Cpx	Cpx	Cpx	Cpx	Cpx	Cpx	Cpx	Amph	Amph	Amph	Amph	Amph
Sample	Tx-36	Tx-36	T-250A	T-268	T-242	Tx-70	Tx-33	Tx-33	Tx-33	T-250A	T-206	T-268	Tx-36	Tx-33	Tx-33	Tx-36
Rock	And	And	Bas	Bas	Bas	Bas	And	And	And	Bas	Bas	Bas	And	And	And	And
	C	M	C	C	C	C	C	C	C	B	M	C	C	C	C	C
SiO2	59.17	58.87	52.48	52.12	52.11	52.85	53.44	52.02	53.12	49.73	47.10	41.11	41.28	43.56	44.10	45.28
Al2O3	25.76	25.28	3.25	3.80	2.64	1.86	2.13	2.96	1.14	4.98	6.36	14.30	13.79	10.50	9.05	7.86
TiO2	-	-	0.53	0.39	0.58	0.63	0.44	0.47	0.30	1.08	2.80	2.14	4.05	2.59	2.62	2.19
FeO	0.19	0.09	4.49	3.92	7.77	10.15	5.65	7.35	10.45	6.14	9.38	8.81	10.38	13.20	14.55	18.34
MgO	-	-	16.60	16.40	16.42	16.30	17.24	15.47	13.73	15.04	12.63	14.53	13.66	13.97	13.25	11.00
CaO	8.06	7.71	22.36	22.90	20.46	18.35	19.97	21.06	20.25	21.41	21.17	12.12	11.90	10.67	11.13	11.00
MnO	-	-	0.20	-	0.03	0.23	0.07	0.03	0.34	0.15	0.16	0.12	0.09	0.28	0.42	0.30
Cr2O3	-	-	0.60	0.26	-	0.09	0.10	0.40	-	0.30	0.03	0.04	-	-	-	-
Na2O	5.98	6.29	0.30	0.19	0.31	0.22	0.26	0.25	0.51	0.29	0.49	2.01	2.36	2.51	2.28	0.72
K2O	0.59	0.64	-	-	-	-	-	-	-	-	-	0.93	1.18	0.61	0.73	0.72
Total	99.74	99.47	100.98	99.98	100.32	100.68	99.33	100.09	99.84	99.17	100.12	96.11	98.69	97.89	98.13	98.52
Si	2.647	2.641	1.905	1.903	1.918	1.947	1.960	1.920	1.987	1.851	1.770	6.082	6.010	6.424	6.543	6.773
Al	1.358	1.368	0.139	0.164	0.115	0.081	0.092	0.129	0.050	0.218	0.282	2.495	2.367	1.826	1.583	0.620
Ti	-	-	0.014	0.011	0.016	0.017	0.012	0.013	0.008	0.030	0.079	0.238	0.443	0.287	0.292	0.246
Fe	0.007	0.003	0.136	0.120	0.239	0.313	0.173	0.227	0.327	0.191	0.295	1.090	1.264	1.628	1.805	2.294
Mg	-	-	0.898	0.893	0.901	0.895	0.943	0.851	0.765	0.835	0.708	3.204	2.964	3.071	2.930	2.452
Ca	0.386	0.371	0.870	0.896	0.807	0.724	0.785	0.833	0.812	0.854	0.852	1.921	1.856	1.686	1.769	1.763
Mn	-	-	0.006	-	0.001	0.007	0.002	0.001	0.011	0.005	0.005	0.015	0.011	0.035	0.053	0.038
Cr	-	-	0.017	0.008	-	0.003	0.003	0.012	-	0.009	0.001	.005	-	-	-	-
Na	0.518	0.547	0.021	0.013	0.022	0.016	0.018	0.018	0.037	0.021	0.036	0.577	0.666	0.718	0.656	0.528
K	0.034	0.037	-	-	-	-	-	-	-	-	-	0.176	0.219	0.115	0.138	0.137
Total	4.950	4.967	4.011	4.008	4.019	4.003	3.989	4.006	3.997	4.015	4.028	15.805	15.804	15.790	15.769	15.618
Na	55.3	57.3														
Ca	41.2	38.8														
K	3.5	3.9														
Ca			45.5	46.9	41.5	37.3	41.3	43.6	42.4	45.3	45.9					
Mg			47.0	46.8	46.2	46.2	49.5	44.5	40.0	44.3	28.0					
Fe			7.5	6.3	12.3	16.5	9.2	11.9	17.6	10.4	16.1					
AlIV			0.095	0.097	0.082	0.053	0.040	0.080	0.013	0.149	0.230	1.917	1.989	1.576	1.457	1.227
AlVI			0.044	0.067	0.033	0.028	0.052	0.049	0.037	0.069	0.052	0.578	0.378	0.250	0.126	0.159
(Na+K)A												0.752	0.805	0.792	0.770	0.620

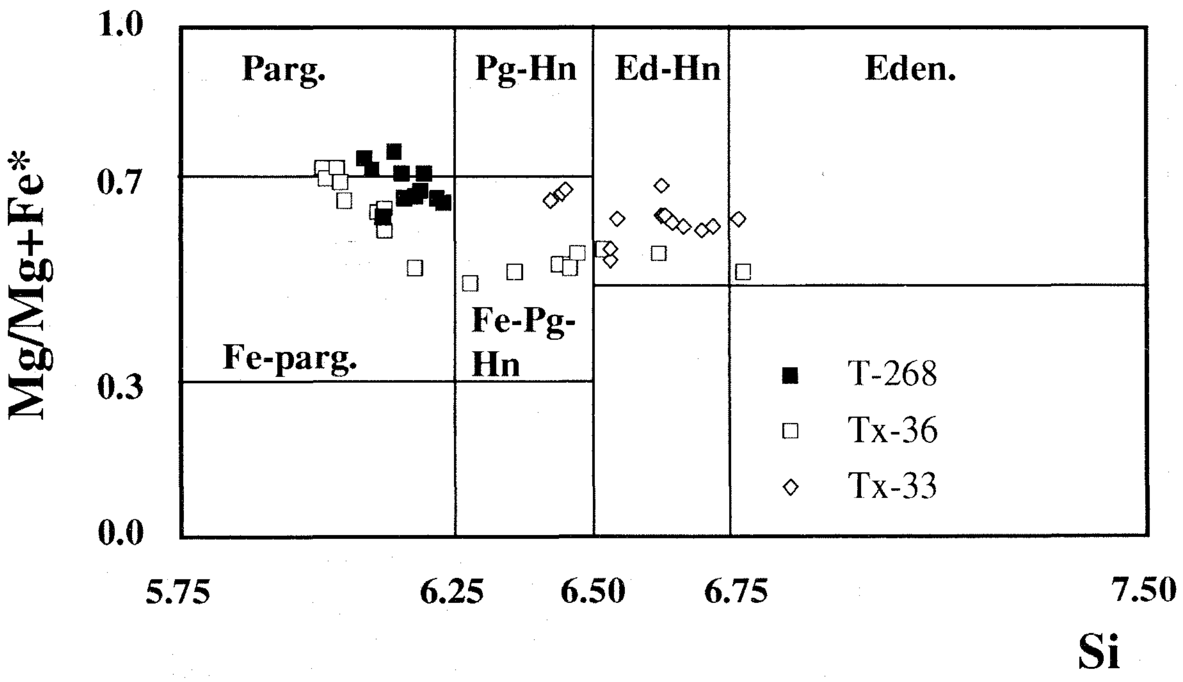

Fig. 8. Magmatic amphibole compositions of basalts (T-268) and andesites (Tx-33, Tx-36) in the classification scheme of Leake (1978).

lavas might be due, at least in part, to low-grade hydrothermal metamorphism. Variations in LIL elements are particularly evident in the multi-element patterns shown in Figure 9. Basic to intermediate lavas (Figure 9a to 9d) were normalized using MORB values of Pearce (1983), whereas acidic lavas (Figure 9e) were normalized using ORG values of Pearce *et al.* (1984). Although all basic to intermediate lavas are highly enriched in LFSE relative to HFSE, the degree of enrichment in rocks with similar mineralogy and HFSE contents is rather chaotic (Figure 6, a-d). A marked negative anomaly in the so-called orogenic elements Nb, Zr and Ti is observed in all basic to intermediate lavas typical of subduction-related magmas. These patterns are similar to those observed in hydrothermally altered calc-alkaline and shoshonite suites from island-arc and calc-alkaline rocks from active continental margins (Pearce, 1983; Morrison, 1980). The two rhyolitic samples shown in Figure 9e display contrasting multi-element patterns. M-14 shows an important enrichment in LFSE and depletion in HFSE relative to ORG, whereas rhyolite M-12 is fairly depleted in all LILE with the exception of Nb, which is higher and Rb and Ce, which are similar to ORG. Since rhyolites are the last products of magmatic differentiation and are also affected by low-grade hydrothermal metamorphism, it is difficult to establish in detail if the observed differences resulted from primary, magmatic or secondary, metamorphic processes. At any rate, rhyolite patterns are strikingly comparable to those observed in island-arc rhyolites. In particular, LFSE-depleted acidic rocks have been recorded in some primitive, tholeiitic intra-oceanic island arcs whereas LFSE-enriched rhyolites are typical of evolved, calc-alkaline suites (*e.g.*, Gill, 1981; Lapierre *et al.* 1992)

Compared to calc-alkaline suites from entirely intra-oceanic island-arc, *i.e.*, island arcs on normal oceanic crust like the Mariana arc (Dixon and Batiza, 1979; Meijer and Reagan, 1981; Bloomer *et al.*, 1989; Lin *et al.*, 1989) or the Aleutian arc (Perfit *et al.*, 1980; Myers *et al.*, 1986), Teloloapan basic to intermediate lavas appear to be enriched in HFS elements such as Y (23.6-36.29 ppm), Zr (99-174 ppm), Nb (3.4-11.6 ppm), HREE ($1.99<\mathrm{Yb}<2.84$ ppm) and to a lesser degree in TiO_2 (1.11-1.41% in basalts). Ratios of HFSE and HREE such as Zr/Y, Ti/V, Sm/Nd and La/Ce are also slightly higher (Table 2). These concentrations and ratios are similar to those found in some medium- to high-K calc-alkaline suites with similar degree of differentiation from evolved island arcs [*e.g.*, the Indonesian arc (Whitford *et al.*, 1977, 1979; Whitford and Jezek, 1979; Stolz *et al.*, 1990); the Lesser Antilles arc (Brown *et al.*, 1977; Hawkesworth and Powell, 1980)], and in unusual island-arc shoshonites [*e.g.*, the Northern Mariana arc (Lin *et al.*, 1989)]. The variations in HFSE and HREE from basalts to andesites (Y and HREE decrease and Zr increases with increasing SiO_2) are consistent with a magmatic evolution by extraction of observed phases (*i.e.*, olivine, pyroxenes, plagioclase, Fe-Ti oxides and amphibole) as previously described.

Teloloapan lavas also feature high absolute REE abundances (La = 69-126; Yb = 11-20 times chondritic). Globally, basalts have the highest REE abundances, whereas rhyolites have the lowest. The chondrite-normalized REE patterns (Figure 10) show that basic to intermediate lavas (Figure 10a to 10d) are all strongely enriched in LREE [$(\mathrm{La/Yb})_N$ = 5.6 to 10.0] relative to HREE, which is typical, in orogenic suites, of medium- to high-K calc-alkaline magmatic series (Gill, 1981). LREE in andesites are slightly higher compared to those of phyric basalts whereas that the HREE are contrarily lower. Rhyolites REE patterns (Figure 10e) show also an important enrichment in LREE relative to HREE although clearly less than in some basalts and andesites [$(\mathrm{La/Yb})_N$ = 3.5 to 5.3]. A negative anomaly in Eu observed in some lavas, particularly in the most fractionated ones, may be the result of fractionation of plagioclase. The differences observed in the absolute REE abundances as well as in the degree of LREE enrichment among basalts, andesites and rhyolites would suggest, according to Gill (1981) and Henderson (1984), that Teloloapan lavas may not be derived from a common co-genetic liquid in spite of observed element-SiO_2 correlation. As we will see later, differences in isotopic composition recorded between basalts and andesites are consistent with this interpretation.

Nd and Sr isotopic data from selected samples including two andesites are listed in Table 3 together with the concentrations of SiO_2. Because of magmatic differentiation, acidic products generally do not show the chemistry of parental magmas. Hence, rhyolitic members were not isotopically analyzed in this study. Initial ratios of ε_{Nd} and ε_{Sr} were calculated at T = 108 Ma (Aptian-Albian boundary) using normalizing values and procedures suggested by De Paolo (1979). The ε_{Nd} and ε_{Sr} values of Teloloapan rocks are plotted in Figure 11 together with available data of some calc-alkaline series from both island arcs and active continental margins for comparison and further discussion.

The range of Nd isotopic composition in Teloloapan lavas is relatively small, ε_{Nd} = +1.6 to +4.6 compared to the larger range observed in Sr isotopic compositions, ε_{Sr}= -14.3 to +2.3. The ε_{Nd} values are much lower than those of MORB but they lie within the range observed in IAB and OIB. Despite the enrichment in radiogenic Sr expected for alteration by the low-grade, hydrothermal metamorphism, ε_{Sr} ratios are relatively low and all samples plot within the mantle array with the exception of one andesite which has the lowest ε_{Sr} and plot in the left side. There is no apparent correlation between ε_{Nd} and ε_{Sr}. Neither do ε_{Nd} or ε_{Sr} correlate with SiO_2 contents. In detail, small but significant differences exist in ε_{Nd} between andesites and associated phyric basalts; andesites tend to exhibit unusually high ε_{Nd} values.

As a group, ε_{Nd} values of Teloloapan lavas are relatively low compared to those of entirely intra-oceanic calc-alkaline series [*e.g.*, the Mariana arc (Lin *et al.*, 1990); the Aleutian arc (McCulloch and Perfit, 1981; Morris and Hart, 1983; Kay *et al.*, 1986)], which systematically have high ε_{Nd} ratios (+6 to as high as +10). Such values are,

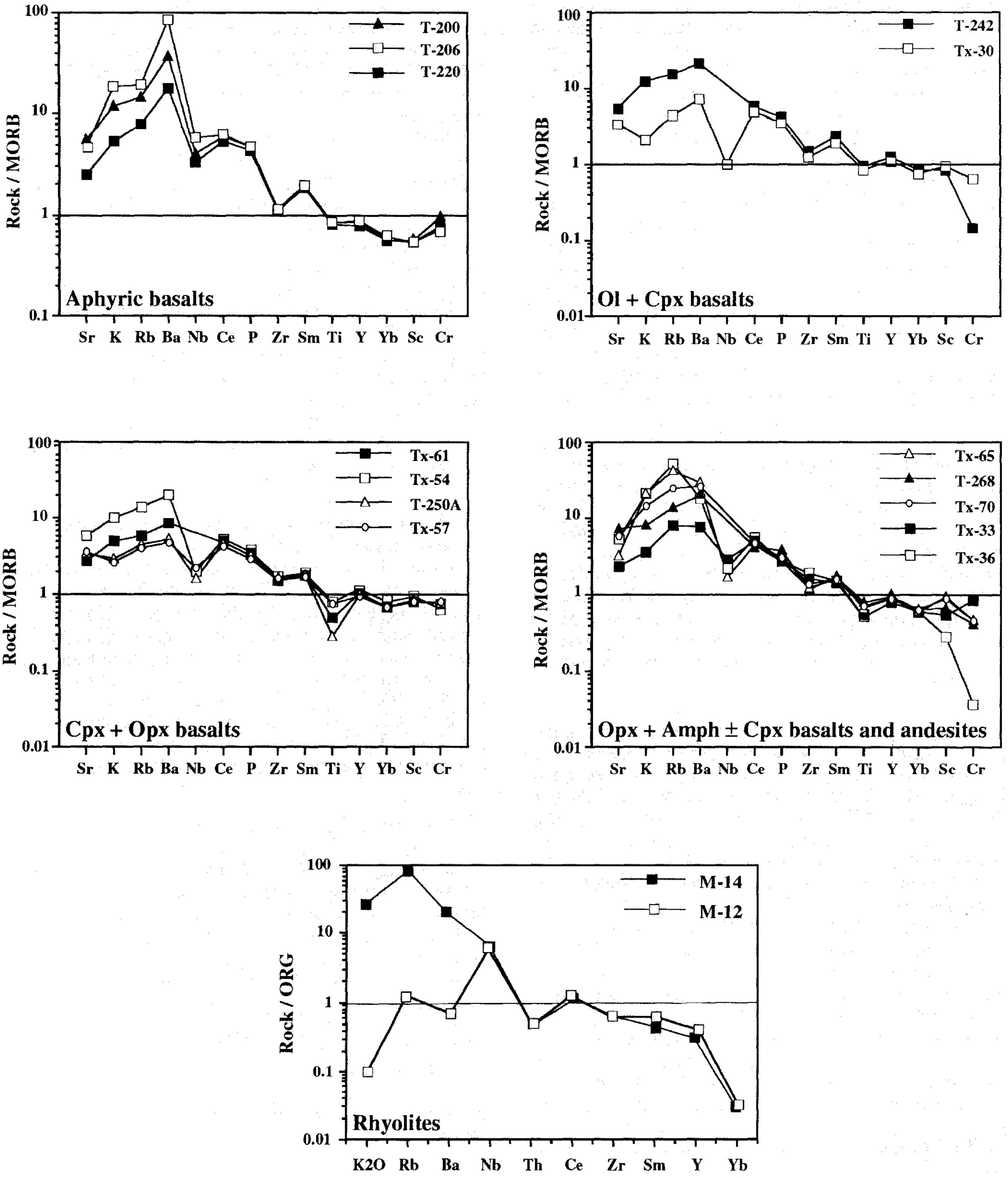

Fig. 9. MORB-normalized multi-element patterns for the Teloloapan lavas. Basic to intermediate lavas were normalized using MORB values of Pearce (1983). Acidic rocks were normalized using ORG values of Pearce *et al.* (1984).

however, common in OIB and in some medium- to high-K calc-alkaline rocks of evolved island arcs [*e.g.*, the Lesser Antilles arc (Hawkesworth and Powell, 1980); the Indonesian arc (Whitford *et al.*, 1979; Stolz *et al.*, 1990)]; some

Table 2

Major, trace and rare earth elements chemistry of lavas of the Teloloapan calc-alkaline suite.

Sample	Tx-61	Tx-54	T-268	T-242	T-206	T-200	T-220	Tx-65	Tx-30	T-250A	Tx-57	Tx-70	Tx-33	Tx-36	M-14	M-12
Rock type	Basalt	Basalt	Basalt	Basalt	Basalt	Basalt	Basalt	Basalt	Basalt	Basalt	Basalt	Basalt	Andesite	Andesite	Rhyolite	Rhyolite
SiO2	46.47	46.79	47.42	47.70	47.87	48.42	49.09	49.09	49.12	49.79	51.20	52.70	56.47	57.65	70.03	73.96
TiO2	1.18	1.23	1.18	1.41	1.25	1.26	1.2	1.03	1.29	1.16	1.12	1.11	0.80	0.81	0.12	0.26
Al2O3	16.46	18.16	18.45	17.23	17.48	17.67	17.64	16.58	15.61	16.32	15.53	16.57	16.71	17.03	12.30	12.53
Fe2O3 †	7.93	9.05	9.13	10.69	8.55	8.35	8.39	9.61	10.8	9.21	8.69	8.33	7.69	6.75	2.53	0.55
MnO	0.10	0.10	0.10	0.12	0.13	0.13	0.15	0.12	0.13	0.08	0.08	0.12	0.08	0.08	0.01	0.01
MgO	4.99	5.72	4.87	5.47	6.24	5.62	4.82	6.71	6.61	5.5	5.47	4.80	3.66	1.75	1.20	0.10
CaO	11.86	8.88	10.42	8.08	8.85	6.85	6.5	6.05	7.95	10.17	9.74	8.33	3.58	5.98	9.98	0.04
Na2O	3.12	3.08	1.87	2.63	1.98	3.52	5.22	3.08	4.25	2.42	2.63	2.24	7.44	3.00	0.40	0.08
K2O	0.60	1.47	1.22	1.81	1.81	2.79	1.2	3.11	0.32	0.44	0.40	2.16	0.55	3.16	0.01	11.05
P2O5	0.40	0.44	0.46	0.51	0.56	0.56	0.53	0.34	0.43	0.38	0.35	0.36	0.34	0.34	0.04	0.06
L. I.	7.20	5.27	5.04	4.07	5.12	4.37	5.78	4.00	3.57	4.58	4.48	3.28	2.46	2.68	3.24	1.08
Total	99.82	99.92	99.89	99.43	99.57	99.26	99.8	99.47	99.8	99.14	99.43	99.64	99.55	99.00	99.86	99.71
Ba	173	404	392	423	746	1713	355	595	144	103	96	512	154	358	35	1015
Rb	12	27	28	30	29	38	16	84	9	9	8	50	16	108	5	342
Sr	327	713	874	664	665	570	294	394	408	414	428	684	290	620	8	5
Sc	33.0	38.2	28.0	33.4	22.29	21.7	21.89	38.5	38.5	33.2	32.4	35.2	22.5	11.8	11.3	5
Co	25	30	32	29	26	25	27	31	30	33	28	28	30	29	5	5
V	206	237	226	310	179	181	177	253	313	213	206	238	157	122	5	22
Ni	55	46	48	30	95	73	80	41	171	56	58	44	82	6	13	5
Cr	189	159	104	36	233	177	194	118	159	194	205	120	217	9	7	5
Nb	-	7**	-	-	14**	20**	11.6*	6.0*	3.4*	5.6*	8**	-	10.1*	7.9*	5**	5**
Y	31.3	34.32	28.71	36.29	24.89	25.78	23.60	26.31	33.31	29.82	29.11	27.47	23.66	23.78	30.13	22.54
Zr	141	151	105	128	104	103	99	113	113	143	135	127	147	174	176	223
La	21.51	23.99	19.15	26.8	28.00	30.68	26.62	20.81	22.00	20.53	19.78	20.58	27.45	28.70	16.86	19.13
Ce	47.97	52.16	43.32	58.59	60.67	63.54	53.30	45.39	50.45	46.61	42.11	46.92	49.37	54.28	38.72	36.69
Nd	25.59	27.23	22.47	33.37	27.97	30.44	28.27	23.70	27.20	24.32	22.95	23.33	22.45	24.90	21.16	17.97
Sm	6.03	6.39	5.52	7.74	6.13	6.57	6.17	5.48	6.24	5.94	5.52	5.25	4.74	5.20	5.27	4.21
Eu	1.54	1.67	1.76	2.06	1.73	1.90	1.68	1.57	1.65	1.51	1.45	1.42	1.23	1.45	0.87	0.75
Gd	5.35	5.66	5.10	6.45	5.28	5.47	4.90	4.77	5.65	5.42	4.94	4.95	3.96	4.31	4.89	3.69
Dy	4.94	5.32	4.61	5.91	4.13	4.27	4.09	4.14	5.26	4.85	4.53	4.35	3.69	3.81	4.88	3.47
Er	2.74	2.97	2.57	3.24	2.29	2.33	2.31	2.28	2.93	2.70	2.46	2.39	2.13	2.29	3.17	2.66
Yb	2.39	2.70	2.26	2.84	1.94	2.06	1.92	2.09	2.67	2.38	2.32	2.21	2.06	2.10	3.25	2.42
Lu	0.29	0.35	0.29	0.36	0.25	0.29	0.23	0.27	0.35	0.29	0.31	0.28	0.25	0.26	0.26	0.43
Mg #	38.6	38.7	34.8	33.8	42.2	40.2	36.5	41.1	38.0	37.4	38.6	36.3	32.2	20.6	32.2	15.4
Zr/Y	4.5	4.4	3.7	3.5	4.2	4.0	4.3	4.2	3.4	4.8	4.6	4.6	6.2	7.3	5.8	9.9
Ti/V	34.4	31.1	31.3	27.3	41.9	41.8	24.4	40.7	24.7	32.7	32.6	28.0	30.6	39.8	144.0	70.9
Sm/Nd	0.24	0.24	0.25	0.23	0.22	0.22	0.22	0.23	0.23	0.24	0.24	0.23	0.21	0.21	0.25	0.23
La/Ce	0.45	0.46	0.44	0.46	0.46	0.48	0.50	0.46	0.44	0.44	0.47	0.44	0.56	0.53	0.44	0.52
(La/Yb)N	6.09	6.01	5.73	6.38	9.76	10.08	9.37	6.73	5.57	5.84	5.77	6.30	9.01	9.24	3.50	5.34

† Total Fe as Fe2O3

* Analyzed by XRF

** Analyzed by ICP-MS

Table 3

Nd and Sr isotopic compositions for select basalts and andesites of the Teloloapan sequence. ε_{Nd} and ε_{Sr} were calculated at T=108 Ma (Aptian-Albian boundary). Normalizing values and procedure are from DePaolo (1979).

Sample	Rock type	SiO2	87Rb/86Sr	87Sr/86Sr	87Sr/86Sr (T)	ESr	147Sm/144Nd	143Nd/144Nd	143Nd/144Nd (T)	ENd
T-206	Aphyric bas	47.87	0.13263	0.704735 ± 22	0.704533	(+) 2,3	0.12182	0.512766 ± 9	0.512680	(+) 3.5
T-250A	Opx-Cpx bas	49.79	0.05045	0.704027 ± 21	0.703851	(-) 6.0	0.13544	0.512745 ± 10	0.512649	(+) 2.9
Tx-70	Opx-Cpx bas	52.70	0.23942	0.704537 ±18	0.704177	(-) 2.8	0.13261	0.512674 ± 12	0.512580	(+) 1,6
Tx-33	Opx-Am and	56.47	0.16265	0.704596 ± 17	0.704352	(-) 0.3	0.11887	0.512821 ± 12	0.512737	(+) 4.6
Tx-36	Opx-Cpx-Am and	57.65	0.53860	0.704180 ± 14	0.703371	(-) 14.3	0.11570	0.512762 ± 9	0.512680	(+) 3.5

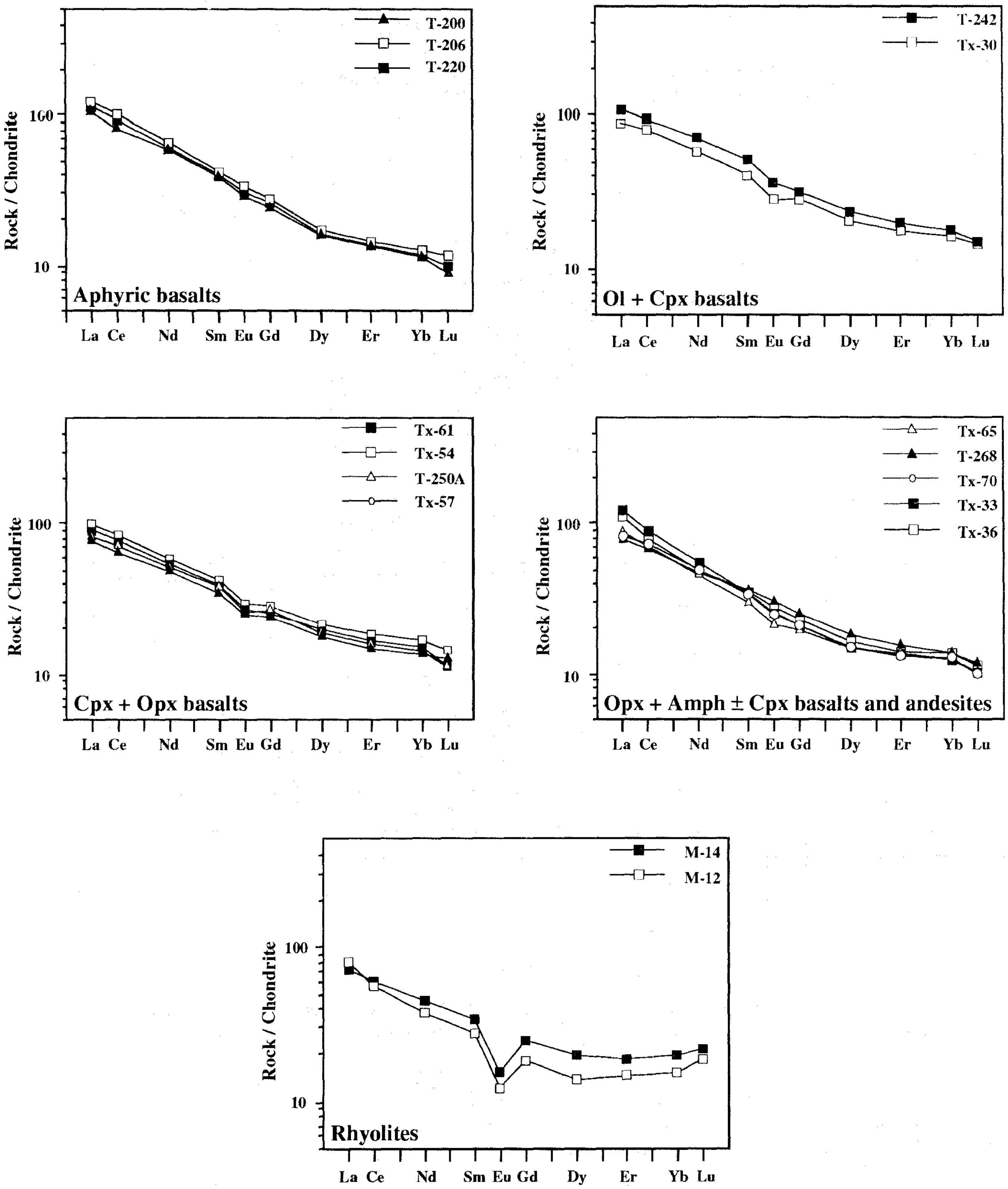

Fig. 10. Chondrite-normalized rare earth patterns for lavas of the Teloloapan subterrane sequence. Normalizing values are from Evensen *et al.* (1978).

active continental margins [*e.g.*, Mexico (Verma and Nelson, 1989) and Ecuador (Hawkesworth *et al.*, 1979)]; and, in unusual intra-oceanic shoshonitic suites [*e.g.*, the Northern Mariana Arc (Lin *et al.*, 1990); Figure 11].

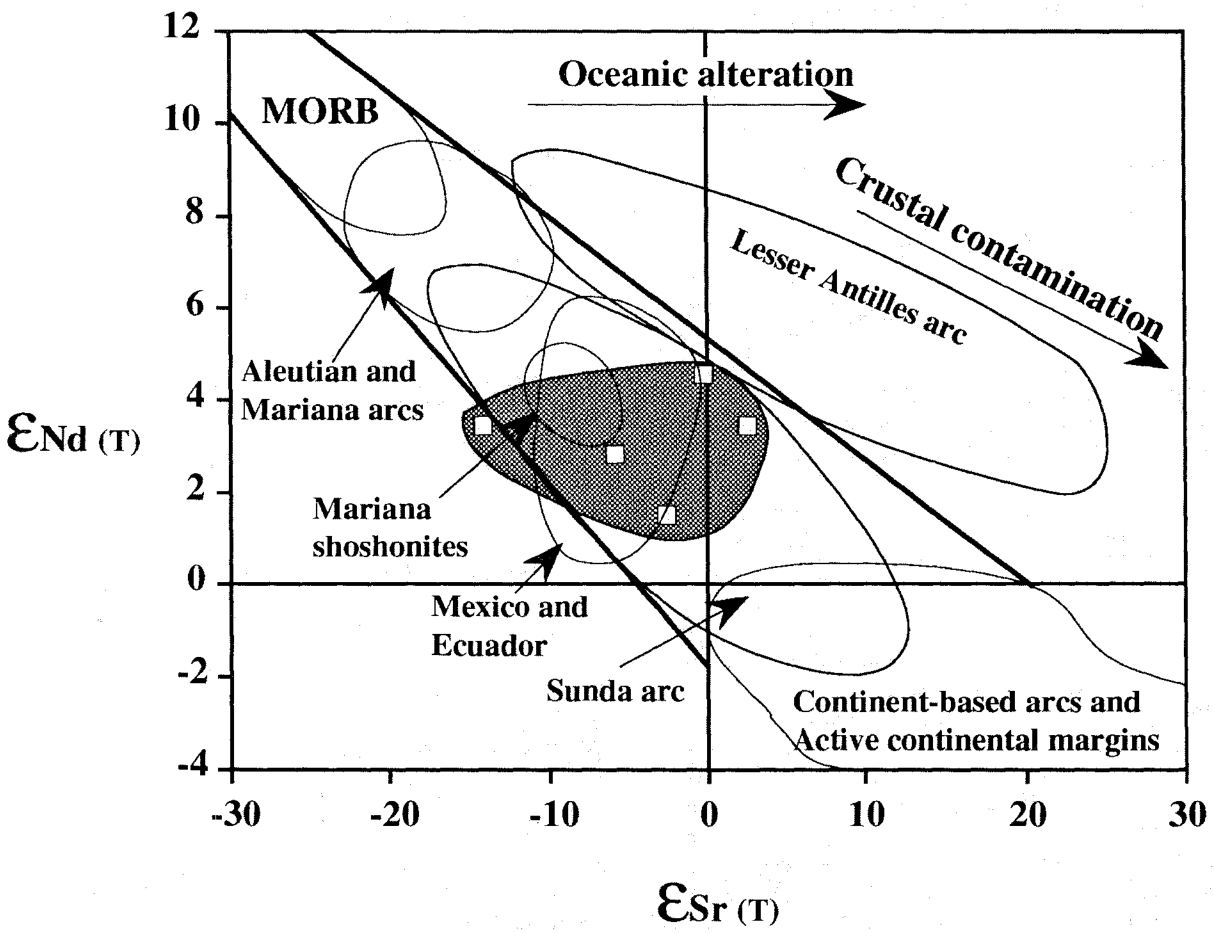

Fig. 11. Diagram ε_{Nd} vs ε_{Sr} ratios comparing Teloloapan calc-alkaline lavas with other suites from some modern island-arc and active continental margins. MORB field and shoshonites from the Mariana arc are also shown. Sources of data are in the text.

DISCUSSION AND CONCLUSIONS

Volcanics in the Teloloapan subterrane sequence constitute a basalt-andesite-rhyolite suite where basalts are largely dominant. Basalts occur throughout the volcanic sequence whereas andesites and rhyolites are restricted to the top stratigraphic levels. Olivine-bearing basalts occur dominantly at the base of the volcanic succession, whereas amphibole-bearing basalts, andesites and rhyolites only occur in the upper levels. This mineralogic evolution is coupled to a decrease in the Mg numbers from bottom to top, suggesting an evolution through time by crystal fractionation. On the other hand, variations recorded in the concentrations of Al_2O_3, Fe_2O_3, TiO_2, MgO, Cr, Ni, V, Y and Zr, especially in basalts, suggest a somewhat extensive fractionation and/or accumulation of the observed phenocryst phases, *i.e.*, olivine, Fe-Ti oxides, clinopyroxene, plagioclase, orthopyroxene and amphibole. The high Al^{IV}/Al^{VI} ratios in clinopyroxenes and the low values of Al^{VI} in mostly amphiboles indicate that fractionation could take place at low pressure, probably at high levels in the crust. There is a negative correlation in the REE abundances and rock types, *i.e.*, among basalts, andesites and rhyolites, and andesites show higher concentrations in Cr and Ni and slightly higher ε_{Nd} ratios than some basalts, this may indicate a different, probably more complex origin for the andesites and rhyolites. According to Gill (1981) and Henderson (1984), these differences might strongly suggest that they could not be related genetically, but are products of different magmatic liquids. Thus, although Teloloapan lavas show a good correlation between SiO_2 and major and some trace elements, they may be derived from different, non cogenetic magmas all having experienced a magmatic evolution involving crystal fractionation and accumulation.

In spite of such differences, basalts and andesites show typical petrographic, mineralogical, geochemical and isotopic characteristics of calc-alkaline suites: (i) presence of two-pyroxene and amphibole basalts and andesites; (ii) early crystallization of Fe-Ti oxides; (iii) clinopyroxene chemistry; (iv) Fe-enrichment trend; (v) high absolute concentrations of LILE and REE; and, (vi) high $((La/Yb)_N)$ ratios. The ε_{Nd} ratios are relatively low. Rhyolites show contrasting LILE and REE abundances relative to basalts and andesites but show also typical magmatic features of island arc suites. The low concentration of MgO, Cr and Ni, together with the low Mg numbers of all lavas including the least differentiated products indicate that analyzed samples represent in fact previously differentiated liquids.

An intra-oceanic origin for the Teloloapan lavas is debatable. The lowest known levels of the sequence are always represented by volcanic rocks and older, crustal rocks have not been mapped in the region (Campa *et al.*, 1974; Campa and Ramírez, 1979; Talavera and Lapierre, 1990; Ruiz *et al.*, 1991; Ortiz *et al.*, 1991). Earlier geochemical and isotopic studies (*e.g.*, Talavera and Lapierre, 1990; Ruiz *et al.*, 1991; Ortiz *et al.*, 1991; Centeno *et al.*, 1992) are consistent with an intra-oceanic origin for the Teloloapan lavas. Campa and Coney (1983) in their description of tectonostratigraphic terranes of Mexico defined the Teloloapan sequence as a volcanic arc subterrane without basement. On the other hand, the presence of a mylonitized granite in the northern part of the subterrane (Parga, 1981) is considered by Elías and Sánchez (1992) as the basement of the Teloloapan arc volcanics. However, the relationships between these rocks and the Teloloapan volcanic rocks are unclear.

Statistical studies on the bulk composition of arc volcanics have been carried out in a great number of island arcs and active continental margins (Gill, 1981 and references therein). This studies indicate that basalts are the typical and most abundant magmatic product in mainly intra-oceanic island arcs, whereas andesites and more differentiated members are typical of continent-based island arcs and mainly active continental margins. On the other hand, the presence of thick ignimbritic deposits and cordierite- and/or garnet-bearing lavas is now considered as typical of mostly continent-based island arcs and active continental margins. In the Teloloapan sequence, geochemical data indicate that volcanics are largely dominated by basalts with scarce andesites and rhyolites at the end of the volcanic activity. Dacitic members were not found. Thick ignimbrite deposits and cordierite-and/or garnet-bearing rocks are missing.

On the other hand, the presence of radiolarian-rich sediments interbedded with pillow-basalts at the base of the volcanic succession indicate a relatively deep environment at the beginning of arc development. Moreover, the presence of pillowed and massive lavas mixed or interbedded with limestones and laminated volcaniclastics at the top of the volcanic pile as well as the absence of subaerial pyroclastic deposits and red beds clearly suggest a completely submerged environment. This inference is strongly supported by the fact that all lavas, even from the uppermost stratigraphic levels, are affected by hydrothermal, seafloor-type metamorphism (Talavera, 1990; Talavera *et al.*, 1993). Thus, sedimentary environments and metamorphic phases are consistent with typical intra-oceanic arc settings.

Finally, continent-based island arc and mostly active continental margin volcanics are typically characterized by low ε_{Nd} values (De Paolo, 1979; Gill, 1981; Faure, 1986), a feature commonly linked to crustal contamination. The ε_{Nd} values of analyzed lavas ($+1.6<\varepsilon_{Nd}<+4.6$), although lower than those reported in calc-alkaline rocks from entirely intra-oceanic island arcs ($+6<\varepsilon_{Nd}<+9$), are significantly higher that those commonly reported in continent-based island arcs and active continental margins ($0>\varepsilon_{Nd}>-10$). ε_{Sr} ratios of lavas are relatively low in spite of the low-grade, hydrothermal metamorphism and all lie or are near the range observed in mantle-derived magmas and show no evidences of sea water nor old crust contribution.

Compared to typical calc-alkaline suites from entirely intra-oceanic island arc, Teloloapan lavas appear to be enriched in both HFSE and REE and exhibit lower ε_{Nd} values. However, similar geochemical and isotopic features have been recorded in lavas from some evolved intra-oceanic island arcs, like the Sunda arc or the Lesser Antilles arc (Whitford *et al.*, 1979; Stolz *et al.*, 1990; Brown *et al.*, 1977; Hawkesworth and Powell, 1980).

In conclusion, the petrographic, geochemical and isotopic evidence in this study strongly suggests that Teloloapan lavas were formed in an evolved intra-oceanic, completely submarine island arc similar to the present-day Sunda arc or Lesser Antilles arc, rather than in a continent-based arc or an active continental margin. Assuming that geochemical and isotopic features of Teloloapan lavas do not involve crustal contamination, we may suggest that they reflect a complex magmatic evolution involving partial melting of a slightly enriched mantle source modified by subducted pelagic sediments, as suggested by several authors for calc-alkaline lavas from the Sunda or Lesser Antilles arc (Whitford *et al.*, 1977; Withford *et al.*, 1981; White and Patchett, 1984; Stolz *et al.*, 1990).

ACKNOWLEDGMENTS

This research is part of the Ph. D. dissertation of the first author (OTM) at the Institut Dolomieu, Université J. Fourier, Grenoble, France. OTM is grateful to H. Lapierre for discussions throughout the project. Comments by H. Lang and an anonymous reviewer are gratefully acknowledged. Support was provided by a grant of SEP-CONACYT, Mexico, and by a «DBT-INSU programme» of France («Thème Dynamique globale»).

BIBLIOGRAPHY

ALIBERT, C., A. MICHARD and F. ALBAREDE, 1983. The transition from alkali basalts to kimberlites: Isotope and trace element evidence from melilite. *Contrib. Mineral. Petrol., 82,* 176-186.

AOKI, K. and I. KUSHIRO, 1968. Some clinopyroxenes from ultramafic inclusions in Dreiser Weiher, Eifel. *Contrib. Mineral. Petrol., 18,* 326-337.

BASALTIC VULCANISM STUDY PROJECT 1981. Basaltic vulcanism on the terrestrial planets. Pergamon, New York, 1286p.

BLOOMER, S. H., R. J. STERN, E. FISK and C. H. GESCHWIND, 1989. Shoshonitic volcanism in the Northern Mariana arc. 1. Mineralogic and major and trace element characteristics. *J. Geophys. Res., 94,* 4469-4496.

BONEAU, M. 1976. A propósito de la edad cretácica de los afloramientos volcánicos y volcaniclásticos de la región de Zihuatanejo, Guerrero (Sierra Madre del Sur, México). III Cong. Latino-americano de Geol., México, Abstracts, p. 14.

BROWN, G. M., J. G. HOLLAND, H. SIGURDSSON, J.F. TOMBLIN and R.J. ARCULUS, 1977. Geochemistry of the Lesser Antilles volcanic island arc. *Geochim. Cosmochim. Acta, 41,* 785-801.

CAMPA, M. F., M. CAMPOS, R. FLORES and R. OVIEDO, 1974. La secuencia mesozoica volcánica-sedimentaria metamorfizada de Ixtapan de la Sal, Méx.-Teloloapan, Gro. *Bol. Soc. Geol. Mex., 35,* 7-28.

CAMPA, M. F., R. OVIEDO and M. TARDY, 1976. La cabalgadura laramídica del dominio volcano-sedimentario (Arco de Alisitos-Teloloapan) sobre el miogeosinclinal mexicano en los límites de los estados de Guerrero y México. III Cong. Latino-americano de Geol., México, Abstracts, p. 23.

CAMPA, M. F. and J. RAMIREZ, 1979. La evolución geológica y la metalogénesis del noroccidente de Guerrero. Serie Técnico-científica, 1, 71p.

CAMPA, M. F., J. RAMIREZ, R. FLORES and P. CONEY, 1981. Terrenos tectonoestratigráficos de la Sierra Madre del Sur, región comprendida entre los Estados de Guerrero, Michoacán, México y Morelos. Serie Técnico-científica, 10, 28p.

CAMPA, M. F. and P. CONEY, 1983. Tectono-stratigraphic terranes and mineral resources distributions in Mexico. *Can. J. Earth Sci., 20,* 1040-1051.

CENTENO, G. E., J. RUIZ, P. J. CONEY, P. J. PATCHETT and G. F. ORTEGA, 1993. Guerrero Terrane of Mexico: its role in the southern Cordillera from new geochemical data. *Geology, 21,* 419-422.

CONEY, P. J. and M.F. CAMPA, 1984. Lithotectonic Terrane Map of Mexico (West of the 91st meridian) MF-1874-D. Departement of the interior U. S. Geol. Survey.

DAVILA, V.M. and M. GUERRERO, 1990. Una edad basada en radiolarios para la secuencia volcánica-sedimentaria de Arcelia, Edo. de Guerrero. X Conv. Geol. Nal. Soc. Geol. Mex., Abstracts, p. 83.

DE CSERNA, Z., N. PALACIOS and A. PANTOJA, 1978. Relaciones de facies de las rocas cretácicas en el noroeste de Guerrero y en áreas colindantes de México y Michoacán. *Bol. Inst. Geol., 2,* 8-18

DE CSERNA, Z. and C. FRIES, 1981. Hoja Taxco 14Q-h (7) con resumen de la geología de la Hoja Taxco, Estados de Guerrero, México y Morelos. Univ. Nal. Autón. México, Inst. Geol. Carta Geológica de México, serie 1:100 000, mapa con texto, 47p.

DELGADO, A. L., M. M. LOPEZ, D. YORK and C. M. HALL, 1990. Geology and geochronology of ultramafic localities in the Cuicateco and Tierra Caliente Complexes, southern Mexico. Geol. Soc. Am. Annual Meet., Abst. with Progr., 326 p.

DePAOLO, D. J. 1979. Implications of correlated Nd and Sr isotopic variations for the chemical evolution of the crust and mantle. *Earth Planet. Sci. Lett., 43,* 201-211.

DIXON, T.H. and R. BATIZA, 1979. Petrology and chemistry of recent lavas in the Northern Marianas: Implications for the origin of island arc basalts. *Contrib. Mineral. Petrol., 70,* 167-181.

ELIAS, H. M. and Z. J. SANCHEZ, 1992. Tectonic implications of a milonitic granite in the lower structural levels of the Tierra Caliente Complex (Guerrero State, Southern Mexico). *Rev. Inst. Geol. UNAM, 9,* 113-125.

EVENSEN, N.M., P.J. HAMILTON and R.K. O'NIONS, 1978. Rare earth abundances in chondritic meteorites. *Geochim. Cosmochim. Acta, 42,* 1199-1212.

FAURE, G. 1986. Principles of isotopic geology. - John Willey & Son, 589p.

FRIES, C. 1960. Geología del Estado de Morelos y de partes adyacentes de México y Guerrero, Región Central Meridional de México. *Inst. Geol. Bull., 60,* 236p.

GILL, J. B. 1981. Orogenic andesites and plate-tectonics. Minerals and Rocks, 16, 390p.

GUERRERO, M., J. RAMIREZ and O. TALAVERA, 1990. Estudio estratigráfico del arco volcánico Cretácico inferior de Teloloapan, Guerrero. X Conv. Geol. Nal. Soc. Geol. Mex., Abstracts, 67.

GUERRERO, M., J. RAMIREZ, O. TALAVERA and M. F. CAMPA, 1991. El desarrollo carbonatado del Cretácico inferior asociado al arco de Teloloapan, Noroccidente del Estado de Guerrero. Conv. Evol. Geol. de México. Soc. Mex. Mineral., Abstracts, 67.

GUERRERO, S.M., M.O. TALAVERA, E.J. RAMIREZ and F. J. RODRIGUEZ, 1993. Estratigrafía y características de depósito del conjunto petrotectónico de Teloloapan, Terreno Guerrero, Mexico. Proceedings of the First Circum-Pacific and Circum-Atlantic Terrane Conference, p. 61-63.

HAMMARSTROM, J.M. and E. ZEN, 1986. Aluminium in hornblende: an empirical igneous geobarometer. *Am. Mineral., 71,* 1297-1313.

HAWKESWORTH, C. J., M. J. NORRY, J. C. RODDICK and P. E. BAKER, 1979. ^{143}Nd/^{144}Nd, ^{87}Sr/^{86}Sr, and incompatible element variation in calc-alkaline andesites and plateau lavas from South America. *Earth Planet. Sci. Lett., 42,* 45-57.

HAWKESWORTH, C.J. and M. POWELL, 1980. Magma genesis in the Lesser Antilles island arc. *Earth Planet. Sci. Lett., 51,* 297-308.

HENDERSON, P. 1982. Rare earth elements geochemistry. Dev. in Geochemistry, 2, 510 p.

HOLLISTER, L. S., G. C. GRISSOM, E. K. PETERS, H.H. STOWELL and V. B. SISSON, 1987. Confirmation of the empirical correlation of Al in hornblende with pressure of solidification of calc-alkaline plutons. *Am. Mineral., 72,* 231-239.

JAKES, P. and A. J. R. WHITE, 1972. Hornblendes from calc-alkaline volcanic rocks of island arcs and continental margins. *Am. Mineral., 57,* 887-902.

KAY, R. W., J. L. RUBENSTONE and M. KAY, 1986. Aleutian terranes from Nd isotopes. *Nature, 332,* 605-609.

LAPIERRE, H., H. E. ORTIZ, W. ABOUCHAMI, O. MONOD, CH. COULON and J. L. ZIMMERMAN, 1992. A Crrustal section of an intra-oceanic island arc - The late Jurassic-Early Cretaceous Guanajuato magmatic sequence (Central Mexico). *Earth Planet. Sci. Lett., 108,* 61-77.

LAPIERRE, H., M. TARDY, C. COULON, E. ORTIZ, J.-L. BOURDIER, J. MARTINEZ and C. FREDYDIER, 1993. Caractérisation, genèse et évolution géodynamique du "Guerrero terrane" (Mexique occidental). *Can. J. Earth Sci.,* (in press).

LEAKE, B. E. 1978. Nomenclature of amphiboles, copiled for subcommittee on amphiboles, International Mineralogical Association. *Mineral. Mag., 42,* 533-563.

LETERRIER, J., R. MAURY, P. THONON, D. GIRARD and M. MARCHAL 1982. Clinopyroxene composition as a method of identification of magmatic affinities of paleo-volcanic series. *Earth Planet. Sci. Lett., 59,* 139-154.

LIN, P., R. J. STERN and S. H. BLOOMER, 1989. Shoshonitic volcanism in the Northern Mariana arc. 2. Large-ion litophile and rare earth element abundances: Evidence for the source of incompatible element enrichments in intraoceanic arcs. *J. Geophys. Res., 94,* 4497-4514.

LIN, P. N., R. J. STERN, J. MORRIS and S. H. BLOOMER, 1990. Nd- and Sr-isotopic compositions of lavas from northern Mariana and southern Volcano arcs: implication for the origin of island arc melts. *Contrib. Mineral. Petrol., 105,* 381-392.

McCULLOCH, M.T. and M.R. PERFIT, 1981. ^{143}Nd/^{144}Nd, ^{87}Sr/^{86}Sr and trace element contraints on the petrogenesis of Aleutian island arc magmas. *Earth Planet. Sci. Lett., 56,* 167-179.

MEIJER, A. and M. REAGAN, 1981. Petrology and geochemistry of Island of Sarigan in the Mariana Arc; Calc-alkaline volcanism in an oceanic setting. *Contrib. Mineral. Petrol., 77,* 337-354.

MICHARD, A., P. GURRIET, M. SOUDANT and F. ALBAREDE, 1985. Nd isotopes in French Phanerozoic shales: External vs internal aspects of crustal evolution. *Geochim. Cosmochim. Acta, 49,* 601-610.

MIYASHIRO, A. 1974. Volcanic rock series in island arcs and active continental margins. *Am. J. Sci., 274,* 321-355.

MIYASHIRO, A. and F. SHIDO, 1975. Tholeiitic and calc-alkalic series in relation to the behaviour of Ti, V, Cr, and Ni. *Am. J. Sci., 275,* 265-277.

MONOD, O., H. SABANERO, J. RAMIREZ and O. TALAVERA, 1992. Laramide tectonics in Ixtapan de la Sal, Mex. Western Mexico. Geodynamic implications. 13 Geowissenschaftliches Lateinamerika-Kolloquium, Ludwig-Maximilians-Universität München, Abstracts.

MORRIS, J. D. and S. R. HART, 1983. Isotopic and incompatible element contraints on the genesis of island arc volcanics from Cold Bay and Amak Island, Aleutians, and implications for mantle structure. *Geochim. Cosmochim. Acta, 47,* 2015-2030.

MORRISON, 1980. Characteristics and tectonic setting of the shoshonite rock association. *Lithos, 13,* 97-108.

MYERS, J.D., B.D. MARSH and K. SINHA, 1986. Geochemical and strontium isotopic characteristics of parental Aleutian arc magmas: evidence from the basaltic lavas of Atka. *Contrib. Mineral. Petrol., 94,* 1-11.

NICHOLLS, I. A. and D. J. WHITFORD, 1976. Primary magmas associated with Quaternary volcanism in the western Sunda arc. *In:* JOHNSON R.W., Ed., Volcanism in Australiasia. Amsterdam-Oxford-New York., Elsevier, 77-90.

ORTEGA, G. F, 1981. Metamorphic belts of southern Mexico and their tectonic significance. *Geofis. Int., 20* (3) 177-202.

ORTIZ, L. H. 1992. L'arc intra-océanique allochtone Jurassique supérieur-Crétacé inférieur du domaine cordillerain mexicain ("Guerrero Terrane"): Pétrographie, géochimie et minéralisations associées des segments de Guanajuato et Palmar Chico-Arcelia. Conséquences paléogéographiques pour le Mésozoïque du Mexique. Thèse Univ. J. Fourier, Grenoble I, France, 312p.

ORTIZ, H. E., M. YTA, O. TALAVERA, H. LAPIERRE, O. MONOD and M. TARDY, 1991. Origine intra-pacifique des formations pluto-volcaniques d'arc du Jurassique supérieur-Crétacé inférieur du Mexique centro-méridional. *C. R. Acad. Sci., 312,* 399-406.

PANTOJA, A. J. 1959. Estudio geológico de reconocimiento de la región de Huetamo, Estado de Michoacán. Bol. Cons. Rec. Nat. no Renovables, 50, 36p.

PARGA, J. de J. 1981. Geología del área de Tizapa, Municipio de Zacazonapan, México. M.S. thesis, Fac. Ciencias, UNAM, 135p.

PEARCE, J. A. 1983. Role of the sub-continental lithosphere in magma genesis at active continental margins. *In*: HAWKESWORTH C.J. & NORRY N.J., Ed., Continental basalts and mantle xenoliths. Shiva Publishing Limited, 372p.

PEARCE, J. A., B. W. NIGEL, HARRIS and A. G. TINDLE, 1984. Trace element discrimination diagrams for the tectonic interpretation of granitic rocks. *J. Petrol., 25,* 956-983.

PERFIT, M. R., H. BRUECKNER, J. R. LAWRANCE and R. W. KAY, 1980. Trace element and isotopic variations in a zoned pluton and associated volcanic rocks, Unalaska Island, Alaska; a model for fractionation in the Aleutian calc-alkaline suite. *Contrib. Mineral. Petrol., 73,* 69.

RAMIREZ, E. J., M. F. CAMPA, M. O. TALAVERA and S. M. GUERRERO, 1991. Caracterización de los arcos insulares de la Sierra Madre del Sur y sus implicaciones tectónicas. Cong. Evol. Geol. México, Abstracts, p. 163-166.

RUIZ, J., E. CENTENO, P.J. CONEY, P.J. PATCHETT and G. F. ORTEGA, 1991. El Terreno Guerrero y su posible correlación con el basamento de la región del Caribe. Conv. Evol. Geol. México, Soc. Mex. Mineral.- Inst. Geol. UNAM, Resúmenes, 192-193.

SALINAS, J.C., O. MONOD, M. FAURE and O. TALAVERA, 1992. Nouvelles données structurales sur les chevauchements laramides du SW du Mexique (Etat de Guerrero). 14e Réunion des sciences de la Terre, Toulouse, Soc. Géol. Fr., Resumés, 138.

SATO, H. 1977. Nickel content of basaltic magmas: identification of primary magmas and measure of the degree of olivine fractionation. *Lithos, 10,* 113-120.

SEDLOCK, R. L., G. F. ORTEGA and R. C. SPEED, 1993. Tectonostratigraphic Terranes and tectonic evolution of Mexico. Geol. Soc. America Sp. Paper 278, 153p.

STEWART, D. C. 1975. Crystal clots in calc-alkaline andesites as breakdown products of high-Al amphiboles. *Contrib. Mineral. Petrol., 53,* 195-204.

STOLZ, A. J., R. VARNE, G. R. DAVIES, G. E. WHELLER and J. D. FODEN, 1990. Magma source components in an arc-continent collision zone: The Flores-Lembata sector, Sunda arc, Indonesia. *Contrib. Mineral. Petrol., 105,* 585-601.

TALAVERA, O. 1990. Les séries calco-alcalines de l'Albo-Aptien de Teloloapan (Etat de Guerrero): dernières manifestations volcaniques de l'arc intra-océanique mésozoïque des cordillères nord-américaines. Diplôme d'études approfondies (DEA), Univ. d'Orléans, France, 104p.

TALAVERA, O. 1993. Les formations orogéniques mésozoïques du Guerrero (Mexique méridional). Contribution a la connaissance de l'évolution géodynamique des cordillères mexicaines. Thèse de doctorat de l'Univ. Joseph Fourier-Grenoble I, France, 462p.

TALAVERA, O. and H. LAPIERRE, 1990. Características petrográficas y afinidad magmática del Arco de Teloloapan. X Conv. Geol. Nal., Soc. Geol. Mex., Resúmenes, 93.

TALAVERA, O., J. RAMIREZ and M. GUERRERO, 1993. Low-grade seafloor-type metamorphism in the lower Cretaceous island-arc series of the Teloloapan Terrane, southern Mexico. Congr. Diversidad Mineral. México, Soc. Mex. Mineral., Abstracts, p. 87-90.

TARDY, M. 1980. Contribution à l'étude géologique de la Sierra Madre Orientale du Mexique. Thèse d'État, Univ. P. et M. Curie, Paris, 459p.

TARDY, M., H. LAPIERRE, J. L. BOURDIER, CH. COULON, H. E. ORTIZ and M. YTA, 1993. Intraoceanic setting of the western Mexico Guerrero Terrane-Implications for the Pacific-Tethys geodynamic relationships during the Cretaceous. *Rev. Inst. Geol. UNAM, 10 (2),* 118-128.

VERMA, S. P. and S. A. NELSON, 1989. Isotopic and trace element contraints on the origin and evolution of alkaline and calc-alkaline magmas in the northwestern Mexican Volcanic Belt. *J. Geophys. Res., 94,* 4531-4544.

VIDAL, S. R., M. F. CAMPA, B. BUITRON and G. ALENCASTER, 1980. El conjunto petrotectónico de Zihuatanejo, Gro. - Coalcomán Col. V Conv. Geol. Nal., Soc. Geol. Mex. Abstracts, p. 111-112.

WHITFORT, D. J., W. COMPSTON, I. A. NICHOLLS and M. J. ABBOTT, 1977. Geochemistry of late cenozoic lavas from eastern Indonesia: Role of subducted sediments in petrogenesis. *Geology, 5,* 571-575.

WHITFORT, D.J. and P.A. JESEK, 1979. Origin of Late-Cenozoic lavas from the Banda arc, Indonesia: Trace element and Sr isotope evidence. *Contrib. Mineral. Petrol., 68,* 141-150.

WHITFORT, D.J., I.A. NICHOLLS and S.R. TAYLOR, 1979. Spatial variations in the geochemistry of Quaternary lavas across the Sunda arc in Java and Bali. *Contrib. Mineral. Petrol., 70,* 341-356.

WHITFORD, D. J., W. M. WHITE and P. A. JESEK, 1981. Neodymium isotopic composition of Quaternary island arc lavas from Indonesia. *Geochim. Cosmochim. Acta, 45,* 989-995.

WHITE, W. M. and J. PACHETT, 1984. Hf-Nd-Sr isotopes and incompatible element abundances in island arcs: implications for magma origins and crust-mantle evolution. *Earth Planet. Sci. Letters, 67,* 167-185.

Oscar Talavera Mendoza, Joel Ramírez Espinosa and Martín Guerrero Suástegui
Escuela Regional de Ciencias de la Tierra, Universidad Autónoma de Guerrero, Ap. 197, 40200 Taxco, Gro. México.